

# Sparse Nonnegative CANDECOMP/PARAFAC Decomposition in Block Coordinate Descent Framework: A Comparison Study

Deqing Wang, *Student Member, IEEE*, Fengyu Cong, *Senior Member, IEEE*,  
and Tapani Ristaniemi, *Senior Member, IEEE*

**Abstract**—Nonnegative CANDECOMP/PARAFAC (NCP) decomposition is an important tool to process nonnegative tensor. Sometimes, additional sparse regularization is needed to extract meaningful nonnegative and sparse components. Thus, an optimization method for NCP that can impose sparsity efficiently is required. In this paper, we construct NCP with sparse regularization (sparse NCP) by  $l_1$ -norm. Several popular optimization methods in block coordinate descent framework are employed to solve the sparse NCP, all of which are deeply analyzed with mathematical solutions. We compare these methods by experiments on synthetic and real tensor data, both of which contain third-order and fourth-order cases. After comparison, the methods that have fast computation and high effectiveness to impose sparsity will be concluded. In addition, we proposed an accelerated method to compute the objective function and relative error of sparse NCP, which has significantly improved the computation of tensor decomposition especially for higher-order tensor.

**Index Terms**—Tensor decomposition, CANDECOMP/PARAFAC (CP) decomposition, nonnegative constraint, sparse regularization, block coordinate descent.

## I. INTRODUCTION

NONNEGATIVE tensor decomposition and nonnegative matrix factorization are powerful tools in signal processing and machine learning [1]–[3]. Due to the nonsubtractive property and part-based representation [4], they have been widely applied to hyperspectral unmixing [5], [6], cognitive neuroscience [7], [8], chemometrics [9], [10], and many other areas [2], [11]. Nonnegative CANDECOMP/PARAFAC (NCP) tensor decomposition is an extension of nonnegative matrix factorization (NMF) from two-way to multi-way. NMF and NCP are data factorization/decomposition methods with nonnegative constraints, which are described as follows.

This work was supported in part by the National Natural Science Foundation of China (Grant No. 81471742), in part by the Fundamental Research Funds for the Central Universities [DUT16JJ(G)03] in Dalian University of Technology in China, and in part by the scholarship from China Scholarship Council (No. 201600090043). (*Corresponding author: Fengyu Cong*)

D. Wang and F. Cong are with the School of Biomedical Engineering, Faculty of Electronic Information and Electrical Engineering, Dalian University of Technology, Dalian 116024, China, and also with the Faculty of Information Technology, University of Jyväskylä, Jyväskylä 40100, Finland (e-mail: deqing.wang@foxmail.com; cong@dlut.edu.cn).

T. Ristaniemi is with the Faculty of Information Technology, University of Jyväskylä, Jyväskylä 40100, Finland (e-mail: tapani.e.ristaniemi@jyu.fi).

Manuscript received Month Day, Year; revised Month Day, Year.

**The NMF problem.** Given a nonnegative matrix  $V \in \mathbb{R}^{I_W \times I_H}$  and a positive integer  $R < \min\{I_W, I_H\}$ , NMF is to solve the following minimization problem:

$$\begin{aligned} \min_{W, H} \frac{1}{2} \|V - WH\|_F^2 \\ \text{s.t. } W \geq 0, H \geq 0, \end{aligned} \quad (1)$$

where matrices  $W \in \mathbb{R}^{I_W \times R}$  and  $H \in \mathbb{R}^{R \times I_H}$  are two estimated nonnegative factors.

**The NCP problem.** Given a nonnegative  $N$ th-order tensor  $\mathcal{X} \in \mathbb{R}^{I_1 \times I_2 \times \dots \times I_N}$  and a positive number  $R$ , NCP is to solve the following minimization problem:

$$\begin{aligned} \min_{\mathbf{A}^{(1)}, \dots, \mathbf{A}^{(N)}} \frac{1}{2} \left\| \mathcal{X} - \llbracket \mathbf{A}^{(1)}, \dots, \mathbf{A}^{(N)} \rrbracket \right\|_F^2 \\ \text{s.t. } \mathbf{A}^{(n)} \geq 0 \text{ for } n = 1, \dots, N, \end{aligned} \quad (2)$$

where  $\mathbf{A}^{(n)} \in \mathbb{R}^{I_n \times R}$  for  $n = 1, \dots, N$  are estimated factors on different modes,  $I_n$  is the size on mode- $n$ , and  $R$  can be seen as the selected rank-1 tensor number (initial components number). The estimated factors in Kruskal operator can be represented by sum of  $R$  rank-1 tensors in outer product form:

$$\llbracket \mathbf{A}^{(1)}, \dots, \mathbf{A}^{(N)} \rrbracket = \sum_{r=1}^R \tilde{\mathcal{X}}_r = \sum_{r=1}^R \mathbf{a}_r^{(1)} \circ \dots \circ \mathbf{a}_r^{(N)}, \quad (3)$$

where  $\mathbf{a}_r^{(n)}$  represents the  $r$ th column of  $\mathbf{A}^{(n)}$ .

Both NMF and NCP are non-convex and non-linear optimization problems, therefore finding their global minimums is NP-hard [12]. Conventionally, problems (1) and (2) can be solved in block coordinate descent (BCD) framework [12]–[14], in which each factor is updated alternatively as a subproblem with other factors fixed. These subproblems are usually convex. In NMF case, a lot of optimization methods have been proposed to solve these subproblems. Lee et al. proposed the multiplicative update (MU) method [4], [15], which is the most popular and widely applied method for NMF. Berry et al. introduced the alternating least square (ALS) method in the review paper [16]. Cichocki et al. proposed the hierarchical alternating least squares (HALS) method for large-scale NMF problems [17], [18]. Xu et al. proposed the alternating proximal gradient (APG) method for NMF with detailed mathematical convergence proofs [13]. The same idea as APG was also proposed in [19] for NMF independently, which was called NeNMF. Recently, the alternating direction method of multipliers (ADMM) has been employed for NMF

problems [20], [21]. In addition, the alternating nonnegative least squares (ANLS) method was deeply analyzed in Lin’s seminal paper with strong optimization properties [22], which has a significant influence on NMF. When ANLS method is utilized, the subproblems of NMF appears as the nonnegative least squares (NNLS) problems. Many efficient methods have been devoted to solve the NNLS subproblems, such as Lin’s project gradient method [22], quasi-Newton method [23], [24], active-set method [25], block principal pivoting method [26], inertial projection neural network [27], and proximal function based method [28]. Most of above methods for NMF can be naturally extended to NCP problems [1], [13], [18], [29]–[31].

If no other constraint or regularization is imposed, (1) and (2) with only the nonnegative constraints can be seen as bound-constrained optimization problems [22]. The nonnegative constraints can guarantee physically meaningful results. Sometimes, incorporating specific regularization can yield more interpretable and accurate results, e.g. sparse regularization, orthogonal regularization, smooth regularization [32], manifold regularization [33], [34], and so on. Due to the intrinsic sparsity in many types of data, such as face image data [4], [33], microarray data [25], text data [26], hyperspectral image data [5] and EEG data [35], sparse results are always required in NMF and NCP problems. Nonnegativity constraint will naturally lead to sparsity in the results, but this sparsity in only a side effect, which can’t be controlled to a certain level [36]. Therefore, explicit sparse regularization is needed. In NMF case, many methods has been proposed to impose sparsity by projection or regularization itermis. Hoyer proposed to project all components in NMF factor into vectors that has desired sparsity degree [36], which can be solved by MU or projected gradient methods [37]. However, this method makes all components have the same fixed sparsity degree, which doesn’t reveal the true sparsity distribution in data. On the other hand,  $l_1$ -norm is a conventional and effective sparse regularizer for signal processing [38]. The reason is that for most underdetermined linear equations the minimization problem with  $l_1$ -norm regularization can yield strong sparsity [39]. Consequently,  $l_1$ -norm is a very promising regularization item for NMF and NCP to impose sparsity.

A multitude of works have been devoted to incorporate sparse regularization to NMF [24], [25], [40], [41], but rare works can be found for tensor decomposition. As far as we know, only a few studies had focused on imposing sparsity by  $l_1$ -norm regularization to Tucker decomposition [42]–[44]. In this study, we investigate nonnegative CANDECOMP/PARAFAC (CP) decomposition with sparse regularization, which is abbreviated to “sparse NCP” for convenience. We design the mathematical model of sparse NCP using  $l_1$ -norm as the engine to impose sparsity explicitly. In order to prevent rank deficiency and increase the stability, squared Frobenius norm is also added as an auxiliary regularization. The popular optimization methods of multiplicative update (MU), alternating least squares (ALS), hierarchical altering least squares (HALS), alternating proximal gradient (APG) and alternating nonnegative least squares (ANLS) are employed to solve the sparse NCP model, which are in block coordinate descent framework [12]–[14]. The sparse NCP

implemented by all the above optimization methods are tested on synthetic tensor data and real tensor data, both of which contain third-order and fourth-order case. The abilities of these methods to impose sparsity are carefully compared. We want to mention HALS is a special method that includes normalization constraints on factor matrices in addition to nonnegative constraint. With additional normalization constraints, NMF and NCP no longer remain bounded problems [22]. Despite the drawback of HALS, we still test its performance on the tensor data for imposing sparsity due to its popularity in the past [1], [18].

Data in tensor, especially higher-order tensor (order  $\geq 4$ ), often consist of a huge amount of points, for which the decomposition might process slowly in some limited conditions. The iterating of tensor decomposition is usually terminated by checking the change of objective function value or data fitting, which is sometimes time consuming. A special strategy based on trace of matrix was used to accelerate the calculation of the objective function at each iteration [13], [19]. We extend this strategy to our sparse NCP problem, in which the  $l_1$ -norm sparse regularization and Frobenius regularization items can be easily handled.

The rest of this paper is organized as follows. In Section II, we describe the mathematical model of the designed sparse NCP. Section III elucidates the solutions to sparse NCP model using MU, ALS, HALS, APG, and ANLS method. In Section IV, we introduce our strategy to speed up the computation of sparse NCP. Section V describes the detailed experiments on synthetic and real datasets. Finally, we discuss several key issues related to sparse NCP in Section VI and conclude our paper in Section VI.

## II. SPARSE NONNEGATIVE CANDECOMP/PARAFAC DECOMPOSITION

In this paper, operator  $\circ$  represents outer product of vectors,  $\odot$  represents the Khatri-Rao product,  $*$  represents the Hadamard product that is the elementwise matrix product,  $\langle \rangle$  represents inner product, and  $\llbracket \rrbracket$  represents Kruskal operator.  $\| \cdot \|_F$  denotes Frobenius norm, and  $\| \cdot \|_1$  denotes  $l_1$ -norm. Basics of tensor computation and multi-linear algebra can be found in review [45].

We present the designed sparse nonnegative CANDECOMP/PARAFAC decomposition (sparse NCP) in this section.

Given a nonnegative  $N$ th-order tensor  $\mathcal{X} \in \mathbb{R}^{I_1 \times I_2 \times \dots \times I_N}$  and a positive number  $R$ , we design the sparse NCP as the following minimization problem:

$$\begin{aligned} \min_{\mathbf{A}^{(1)}, \dots, \mathbf{A}^{(N)}} \mathcal{O} &= \frac{1}{2} \left\| \mathcal{X} - \llbracket \mathbf{A}^{(1)}, \dots, \mathbf{A}^{(N)} \rrbracket \right\|_F^2 \\ &+ \sum_{n=1}^N \frac{\alpha_n}{2} \left\| \mathbf{A}^{(n)} \right\|_F^2 + \sum_{n=1}^N \beta_n \sum_{r=1}^R \left\| \mathbf{a}_r^{(n)} \right\|_1 \quad (4) \\ \text{s.t. } \mathbf{A}^{(n)} &\geq 0 \text{ for } n = 1, \dots, N, \end{aligned}$$

where  $\mathbf{A}^{(n)} \in \mathbb{R}^{I_n \times R}$  for  $n = 1, \dots, N$  are the estimated factors in different modes,  $\alpha_n$  and  $\beta_n$  are positive regularization parameters in parameter vectors  $\boldsymbol{\alpha} \in \mathbb{R}^{N \times 1}$  and  $\boldsymbol{\beta} \in \mathbb{R}^{N \times 1}$ ,

$I_n$  is the size in mode- $n$ ,  $\mathbf{a}_r^{(n)}$  represents the  $r$ th column of  $\mathbf{A}^{(n)}$ , and  $R$  is the initial number of components.

Let  $\mathbf{X}_{(n)} \in \mathbb{R}^{I_n \times \prod_{\bar{n}=1, \bar{n} \neq n}^N I_{\bar{n}}}$  represent the mode- $n$  unfolding (matricization) of original tensor  $\mathcal{X}$ . And the mode- $n$  unfolding of the estimated tensor in Kruskal operator  $\llbracket \mathbf{A}^{(1)}, \dots, \mathbf{A}^{(N)} \rrbracket$  can be written as  $\mathbf{A}^{(n)} (\mathbf{B}^{(n)})^T$ , in which  $\mathbf{B}^{(n)} = \left( \mathbf{A}^{(N)} \circ \dots \circ \mathbf{A}^{(n+1)} \circ \mathbf{A}^{(n-1)} \circ \dots \circ \mathbf{A}^{(1)} \right) \in \mathbb{R}^{\prod_{\bar{n}=1, \bar{n} \neq n}^N I_{\bar{n}} \times R}$ . In block coordinate descent framework, factor  $\mathbf{A}^{(n)}$  is updated alternatively by a subproblem in every iteration, which equals to the following minimization problem:

$$\begin{aligned} \min_{\mathbf{A}^{(n)}} \mathcal{F} \left( \mathbf{A}^{(n)} \right) &= \frac{1}{2} \left\| \mathbf{X}_{(n)} - \mathbf{A}^{(n)} (\mathbf{B}^{(n)})^T \right\|_F^2 \\ &+ \frac{\alpha_n}{2} \left\| \mathbf{A}^{(n)} \right\|_F^2 + \beta_n \sum_{r=1}^R \left\| \mathbf{a}_r^{(n)} \right\|_1 \quad (5) \\ \text{s.t. } \mathbf{A}^{(n)} &\geq 0. \end{aligned}$$

As previously mentioned, the sparse NCP problem in (4) is non-convex, therefore finding its global minimum is NP-hard. However, the subproblem (5) with Frobenius norm and  $l_1$ -norm is convex [19], which is the key point to solve (4). All the optimization methods introduced in the introduction can be applied to (5). Furthermore, the objective function in (5) can be represented as

$$\begin{aligned} \mathcal{F} \left( \mathbf{A}^{(n)} \right) &= \frac{1}{2} \text{tr} \left[ \mathbf{X}_{(n)}^T \mathbf{X}_{(n)} \right] - \text{tr} \left[ \left( \mathbf{A}^{(n)} \right)^T \mathbf{X}_n \mathbf{B}^{(n)} \right] \\ &+ \frac{1}{2} \text{tr} \left[ \mathbf{A}^{(n)} \left( \mathbf{B}^{(n)} \right)^T \mathbf{B}^{(n)} \left( \mathbf{A}^{(n)} \right)^T \right] \quad (6) \\ &+ \frac{\alpha_n}{2} \text{tr} \left[ \left( \mathbf{A}^{(n)} \right)^T \mathbf{A}^{(n)} \right] + \beta_n \text{tr} \left[ \mathbf{E}^T \mathbf{A}^{(n)} \right], \end{aligned}$$

where  $\mathbf{E} \in \mathbb{R}^{I_n \times R}$  is a matrix whose elements are all equal to 1. The partial gradient (or partial derivative) of  $\mathcal{F}$  with respect to  $\mathbf{A}^{(n)}$  is always used during computation,

$$\begin{aligned} \nabla_{\mathbf{A}^{(n)}} \mathcal{F} \left( \mathbf{A}^{(n)} \right) &= \frac{\partial}{\partial \mathbf{A}^{(n)}} \mathcal{F} \left( \mathbf{A}^{(n)} \right) \\ &= -\mathbf{X}_{(n)} \mathbf{B}^{(n)} + \mathbf{A}^{(n)} \left( \mathbf{B}^{(n)} \right)^T \mathbf{B}^{(n)} + \alpha_n \mathbf{A}^{(n)} + \beta_n \mathbf{E} \\ &= \mathbf{A}^{(n)} \left[ \left( \mathbf{B}^{(n)} \right)^T \mathbf{B}^{(n)} + \alpha_n \mathbf{I}_R \right] - \mathbf{X}_{(n)} \mathbf{B}^{(n)} + \beta_n \mathbf{E}, \quad (7) \end{aligned}$$

where  $\mathbf{X}_{(n)} \mathbf{B}^{(n)}$  is called the *Matricized Tensor Times Khatri-Rao Product* (MTTKRP) [46]. The item  $\left( \mathbf{B}^{(n)} \right)^T \mathbf{B}^{(n)}$  can be computed efficiently by

$$\begin{aligned} \left( \mathbf{B}^{(n)} \right)^T \mathbf{B}^{(n)} &= \left[ \left( \mathbf{A}^{(N)} \right)^T \mathbf{A}^{(N)} \right] * \dots \\ &* \left[ \left( \mathbf{A}^{(n+1)} \right)^T \mathbf{A}^{(n+1)} \right] * \left[ \left( \mathbf{A}^{(n-1)} \right)^T \mathbf{A}^{(n-1)} \right] \quad (8) \\ &* \dots * \left[ \left( \mathbf{A}^{(1)} \right)^T \mathbf{A}^{(1)} \right]. \end{aligned}$$

### III. OPTIMIZATION METHODS FOR SOLVING SPARSE NCP

In this section, we present the solutions to the sparse NCP problem in (4) by all the optimization methods of MU, ALS,

HALS, APG, and ANLS. To the best of our knowledge, there are no existing solution proposed directly for (4). Some optimization methods had been employed to solve NMF and NCP with Frobenius norm or  $l_1$ -norm regularization item separately [16], [25], [29], [32], so it is natural to combine the solution for these two items together.

#### A. Multiplicative Update

Multiplicative update (MU) was first proposed by Lee et al for NMF [4], [15]. Cai et al. proposed a straightforward way using lagrange multiplier to solve NMF subproblems [33], where the same update rules can be obtained as Lee's method. We extend Cai's method to tensor case. Represent tensor factor  $\mathbf{A}^{(n)}$  elementwisely by  $\mathbf{A}^{(n)} = [a_{ir}^{(n)}]$  for  $i = 1, \dots, I_n$  and  $r = 1, \dots, R$ . Let  $\psi_{ir}$  be the Lagrange multiplier for constraint  $a_{ir}^{(n)} \geq 0$ , and  $\Psi = [\psi_{ir}]$ , based on (6) the Lagrange  $\mathcal{L}$  is

$$\begin{aligned} \mathcal{L} &= \mathcal{F} \left( \mathbf{A}^{(n)} \right) + \text{tr} \left[ \Psi \left( \mathbf{A}^{(n)} \right)^T \right] \\ &= \frac{1}{2} \text{tr} \left[ \mathbf{X}_{(n)}^T \mathbf{X}_{(n)} \right] - \text{tr} \left[ \left( \mathbf{A}^{(n)} \right)^T \mathbf{X}_n \mathbf{B}^{(n)} \right] \\ &+ \frac{1}{2} \text{tr} \left[ \mathbf{A}^{(n)} \left( \mathbf{B}^{(n)} \right)^T \mathbf{B}^{(n)} \left( \mathbf{A}^{(n)} \right)^T \right] \quad (9) \\ &+ \frac{\alpha_n}{2} \text{tr} \left[ \left( \mathbf{A}^{(n)} \right)^T \mathbf{A}^{(n)} \right] + \beta_n \text{tr} \left[ \mathbf{E}^T \mathbf{A}^{(n)} \right] \\ &+ \text{tr} \left[ \Psi \left( \mathbf{A}^{(n)} \right)^T \right]. \end{aligned}$$

The partial derivative of  $\mathcal{L}$  with respect to  $\mathbf{A}^{(n)}$  is

$$\begin{aligned} \frac{\partial \mathcal{L}}{\partial \mathbf{A}^{(n)}} &= -\mathbf{X}_{(n)} \mathbf{B}^{(n)} + \mathbf{A}^{(n)} \left( \mathbf{B}^{(n)} \right)^T \mathbf{B}^{(n)} \\ &+ \alpha_n \mathbf{A}^{(n)} + \beta_n \mathbf{E} + \Psi. \quad (10) \end{aligned}$$

Using KKT condition  $\psi_{ir} a_{ir}^{(n)} = 0$ , we obtain the following equation for  $a_{ir}^{(n)}$ :

$$\begin{aligned} - \left[ \mathbf{X}_{(n)} \mathbf{B}^{(n)} \right]_{ir} a_{ir}^{(n)} + \\ \left[ \mathbf{A}^{(n)} \left( \mathbf{B}^{(n)} \right)^T \mathbf{B}^{(n)} + \alpha_n \mathbf{A}^{(n)} + \beta_n \mathbf{E} \right]_{ir} a_{ir}^{(n)} = 0. \quad (11) \end{aligned}$$

This equation leads to the following multiplicative updating rule:

$$a_{ir}^{(n)} \leftarrow a_{ir}^{(n)} \frac{\left[ \mathbf{X}_{(n)} \mathbf{B}^{(n)} \right]_{ir}}{\left[ \mathbf{A}^{(n)} \left( \left( \mathbf{B}^{(n)} \right)^T \mathbf{B}^{(n)} + \alpha_n \mathbf{I}_R \right) + \beta_n \mathbf{E} \right]_{ir}}, \quad (12)$$

where  $\mathbf{I}_R \in \mathbb{R}^{R \times R}$  is a identity matrix. The implementation of MU method is listed in **Algorithm 1**.

#### B. Alternating Least Squares

Cichochi et al. comprehensively introduced the ALS method to solve NMF and NCP problems with diverse regularization items [1]. ALS method is quite easy to implement for the sparse NCP problem (4).

---

**Algorithm 1:** MU for sparse NCP in (4)
 

---

**Input :**  $\mathcal{X}$ ,  $R$ ,  $\alpha$ ,  $\beta$   
**Output:**  $\mathbf{A}^{(n)}$ ,  $n = 1, \dots, N$   
 1 Initialize  $\mathbf{A}^{(n)} \in \mathbb{R}^{I_n \times R}$ ,  $n = 1, \dots, N$ , using random numbers, then plus a small positive number  $\epsilon$  to all elements;  
 2 **repeat**  
 3     **for**  $n = 1$  **to**  $N$  **do**  
 4         Make mode- $n$  unfolding of  $\mathcal{X}$  as  $\mathbf{X}_{(n)}$ ;  
 5         Compute MTTKRP  $\mathbf{X}_{(n)}\mathbf{B}^{(n)}$  and  $(\mathbf{B}^{(n)})^T \mathbf{B}^{(n)}$  based on (8);  
 6         **for**  $i = 1$  **to**  $I_n$  **do**  
 7             **for**  $r = 1$  **to**  $R$  **do**  
 8                 Update  $a_{ir}^{(n)}$  according to (12);  
 9             **end**  
 10         **end**  
 11     **end**  
 12 **until** some termination criterion is reached;

---

Let the partial derivative of the objective function  $\mathcal{F}(\mathbf{A}^{(n)})$  in (7) equal to 0,

$$\begin{aligned}
 & \frac{\partial}{\partial \mathbf{A}^{(n)}} \mathcal{F}(\mathbf{A}^{(n)}) \\
 &= \mathbf{A}^{(n)} \left[ (\mathbf{B}^{(n)})^T \mathbf{B}^{(n)} + \alpha_n \mathbf{I}_R \right] - \left[ \mathbf{X}_{(n)} \mathbf{B}^{(n)} - \beta_n \mathbf{E} \right] \\
 &= 0,
 \end{aligned} \tag{13}$$

we have the following updating rule for  $\mathbf{A}^{(n)}$ ,

$$\mathbf{A}^{(n)} \leftarrow \left[ \frac{\mathbf{X}_{(n)} \mathbf{B}^{(n)} - \beta_n \mathbf{E}}{(\mathbf{B}^{(n)})^T \mathbf{B}^{(n)} + \alpha_n \mathbf{I}_R} \right]_+, \tag{14}$$

where  $[\ ]_+$  is a half-wave rectifying nonlinear projection to enforce nonnegativity. **Algorithm 2** shows the implementation of ALS method.

---

**Algorithm 2:** ALS for sparse NCP in (4)
 

---

**Input :**  $\mathcal{X}$ ,  $R$ ,  $\alpha$ ,  $\beta$   
**Output:**  $\mathbf{A}^{(n)}$ ,  $n = 1, \dots, N$   
 1 Initialize  $\mathbf{A}^{(n)} \in \mathbb{R}^{I_n \times R}$ ,  $n = 1, \dots, N$ , using random numbers;  
 2 **repeat**  
 3     **for**  $n = 1$  **to**  $N$  **do**  
 4         Make mode- $n$  unfolding of  $\mathcal{X}$  as  $\mathbf{X}_{(n)}$ ;  
 5         Compute MTTKRP  $\mathbf{X}_{(n)}\mathbf{B}^{(n)}$  and  $(\mathbf{B}^{(n)})^T \mathbf{B}^{(n)}$  based on (8);  
 6         Update  $\mathbf{A}^{(n)}$  by  $\mathbf{A}^{(n)} \leftarrow \left[ \frac{\mathbf{X}_{(n)} \mathbf{B}^{(n)} - \beta_n \mathbf{E}}{(\mathbf{B}^{(n)})^T \mathbf{B}^{(n)} + \alpha_n \mathbf{I}_R} \right]_+$ ;  
 7     **end**  
 8 **until** some termination criterion is reached;

---

### C. Hierarchical Alternating Least Squares

Hierarchical alternating least squares (HALS) is a method to update each factor column by column. For the sake of

simplification, we use  $\mathbf{a}_r$  and  $\mathbf{b}_r$  instead of  $\mathbf{a}_r^{(n)}$  and  $\mathbf{b}_r^{(n)}$  in this part, which are the  $r$ th column of  $\mathbf{A}^{(n)}$  and  $\mathbf{B}^{(n)}$  respectively. We also use  $[\mathbf{A}^{(n)}]_{(:,r)} = \mathbf{a}_r \in \mathbb{R}^{I_n \times 1}$  to represent the column of a matrix, and  $[\mathbf{A}^{(n)}]_{(i,r)} = a_{ir}^{(n)}$  to represent an element in a matrix. The objective function  $\mathcal{F}$  in (5) can be represent as

$$\mathcal{F} = \frac{1}{2} \left\| \mathbf{X}_{(n)} - \sum_{r=1}^R \mathbf{a}_r \mathbf{b}_r^T \right\|_F^2 + \frac{\alpha_n}{2} \sum_{r=1}^R \|\mathbf{a}_r\|_2^2 + \beta_n \|\mathbf{a}_r\|_1. \tag{15}$$

The minimization problem in (5) can be solved iteratively by subproblems of columns:

$$\begin{aligned}
 \min_{\mathbf{a}_r} \mathcal{F}_r &= \frac{1}{2} \left\| \mathbf{Z}_r - \mathbf{a}_r \mathbf{b}_r^T \right\|_F^2 + \frac{\alpha_n}{2} \|\mathbf{a}_r\|_2^2 + \beta_n \|\mathbf{a}_r\|_1 \\
 \text{s.t. } & \mathbf{a}_r \geq 0,
 \end{aligned} \tag{16}$$

for  $r = 1, \dots, R$ , and

$$\mathbf{Z}_r = \mathbf{X}_{(n)} - \sum_{\tilde{r}=1, \tilde{r} \neq r}^R \mathbf{a}_{\tilde{r}} \mathbf{b}_{\tilde{r}}^T. \tag{17}$$

The partial derivative of  $\mathcal{F}_r$  with respect to  $\mathbf{a}_r$  is

$$\begin{aligned}
 \frac{\partial \mathcal{F}_r}{\partial \mathbf{a}_r} &= (\mathbf{a}_r \mathbf{b}_r^T - \mathbf{Z}_r) \mathbf{b}_r + \alpha_n \mathbf{a}_r + \beta_n \mathbf{1}, \\
 &= (\mathbf{b}_r^T \mathbf{b}_r + \alpha_n) \mathbf{a}_r - (\mathbf{Z}_r \mathbf{b}_r - \beta_n \mathbf{1}),
 \end{aligned} \tag{18}$$

where  $\mathbf{1} \in \mathbb{R}^{I_n \times 1}$  is a vector with all elements equaling to 1. When  $\frac{\partial \mathcal{F}_r}{\partial \mathbf{a}_r} = 0$ , nonnegative column vector  $\mathbf{a}_r$  can be updated as

$$\mathbf{a}_r \leftarrow \frac{[\mathbf{Z}_r \mathbf{b}_r - \beta_n \mathbf{1}]_+}{\mathbf{b}_r^T \mathbf{b}_r + \alpha_n}, \tag{19}$$

which is a closed-form solution [12].

A fast HALS method was proposed to solve large-scale NMF problem [1], [12]. We use the same idea to solve the sparse NCP problem.  $\mathbf{Z}_r$  in (17) can also be represented as

$$\mathbf{Z}_r = \mathbf{X}_{(n)} - \sum_{\tilde{r}=1}^R \mathbf{a}_{\tilde{r}} \mathbf{b}_{\tilde{r}}^T + \mathbf{a}_r \mathbf{b}_r^T. \tag{20}$$

Replacing  $\mathbf{Z}_r$  in (19) by (20), we obtain the new efficient update rule for  $\mathbf{a}_r$  as is shown in (21).

However, as mentioned above,  $\mathbf{a}_r$  in different factors is usually poorly scaled, therefore after updating in (21) it has to be normalized as

$$\mathbf{a}_r^{(n)} \leftarrow \frac{\mathbf{a}_r^{(n)}}{\left\| \mathbf{a}_r^{(n)} \right\|_2}, \tag{22}$$

for  $n = 1, \dots, N - 1$ , and  $r = 1, \dots, R$ . The procedures of HALS are illustrated in **Algorithm 3**.

### D. Alternating Proximal Gradient

The mathematical properties of alternating proximal gradient (APG) method were thoroughly analyzed in Xu's works [13], [44]. APG method has exhibited excellent performances on both NMF and NCP problems, which is also efficient to

$$\begin{aligned}
 \mathbf{a}_r &\leftarrow \frac{\left[ \left( \mathbf{X}_{(n)} - \sum_{\tilde{r}=1}^R \mathbf{a}_{\tilde{r}} \mathbf{b}_{\tilde{r}}^T + \mathbf{a}_r \mathbf{b}_r^T \right) \mathbf{b}_r - \beta_n \mathbf{1} \right]_+}{\mathbf{b}_r^T \mathbf{b}_r + \alpha_n} = \frac{\left[ \mathbf{X}_{(n)} \mathbf{b}_r - \sum_{\tilde{r}=1}^R \mathbf{a}_{\tilde{r}} \mathbf{b}_{\tilde{r}}^T \mathbf{b}_r + \mathbf{a}_r \mathbf{b}_r^T \mathbf{b}_r - \beta_n \mathbf{1} \right]_+}{\mathbf{b}_r^T \mathbf{b}_r + \alpha_n} \\
 &= \frac{\left[ \left[ \mathbf{X}_{(n)} \mathbf{B}^{(n)} \right]_{(:,r)} - \mathbf{A}^{(n)} \left[ \left( \mathbf{B}^{(n)} \right)^T \mathbf{B}^{(n)} \right]_{(:,r)} + \mathbf{a}_r \left[ \left( \mathbf{B}^{(n)} \right)^T \mathbf{B}^{(n)} \right]_{(r,r)} - \beta_n \mathbf{1} \right]_+}{\left[ \left( \mathbf{B}^{(n)} \right)^T \mathbf{B}^{(n)} \right]_{(r,r)} + \alpha_n} \\
 &= \left[ \frac{\left[ \left( \mathbf{B}^{(n)} \right)^T \mathbf{B}^{(n)} \right]_{(r,r)}}{\left[ \left( \mathbf{B}^{(n)} \right)^T \mathbf{B}^{(n)} \right]_{(r,r)} + \alpha_n} \mathbf{a}_r + \frac{\left[ \mathbf{X}_{(n)} \mathbf{B}^{(n)} \right]_{(:,r)} - \mathbf{A}^{(n)} \left[ \left( \mathbf{B}^{(n)} \right)^T \mathbf{B}^{(n)} \right]_{(:,r)} - \beta_n \mathbf{1}}{\left[ \left( \mathbf{B}^{(n)} \right)^T \mathbf{B}^{(n)} \right]_{(r,r)} + \alpha_n} \right]_+
 \end{aligned} \tag{21}$$

---

**Algorithm 3:** HALS for sparse NCP in (4)
 

---

**Input :**  $\mathcal{X}$ ,  $R$ ,  $\alpha$ ,  $\beta$ 
**Output:**  $\mathbf{A}^{(n)}$ ,  $n = 1, \dots, N$ 

- 1 Initialize  $\mathbf{A}^{(n)} \in \mathbb{R}^{I_n \times R}$ ,  $n = 1, \dots, N$ , using random numbers;
  - 2 **repeat**
  - 3     **for**  $n = 1$  **to**  $N$  **do**
  - 4         Make mode- $n$  unfolding of  $\mathcal{X}$  as  $\mathbf{X}_{(n)}$ ;
  - 5         Compute MTTKRP  $\mathbf{X}_{(n)} \mathbf{B}^{(n)}$  and  $\left( \mathbf{B}^{(n)} \right)^T \mathbf{B}^{(n)}$  based on (8);
  - 6         **for**  $r = 1$  **to**  $R$  **do**
  - 7             Update  $\mathbf{a}_r^{(n)}$  using (21);
  - 8             **if**  $n < N$  **then**
  - 9                 Normalize  $\mathbf{a}_r^{(n)}$  by  $\mathbf{a}_r^{(n)} \leftarrow \frac{\mathbf{a}_r^{(n)}}{\|\mathbf{a}_r^{(n)}\|_2}$ ;
  - 10             **end**
  - 11         **end**
  - 12     **end**
  - 13 **until** some termination criterion is reached;
- 

cope with  $l_1$  sparse regularization [44]. Supposing updating  $\mathbf{A}^{(n)}$  in (4) at the  $k$ th iteration, APG is computed as the following.

Calculate block-partial gradient of  $\mathcal{F}(\mathbf{A}^{(n)})$  in (5) as  $\nabla_{\mathbf{A}^{(n)}} \mathcal{F}(\mathbf{A}^{(n)}) = \frac{\partial}{\partial \mathbf{A}^{(n)}} \mathcal{F}(\mathbf{A}^{(n)})$ . We take

$$L_{k-1}^{(n)} = \left\| \left( \mathbf{B}_{k-1}^{(n)} \right)^T \mathbf{B}_{k-1}^{(n)} \right\|_2 \tag{23}$$

as Lipschitz constant of  $\nabla_{\mathbf{A}^{(n)}} \mathcal{F}$  with respect to  $\mathbf{A}^{(n)}$ , where  $\|\mathbf{A}\|_2$  is spectral norm of matrix. We also select

$$\omega_{k-1}^{(n)} = \min \left( \hat{\omega}_{k-1}, \delta_\omega \sqrt{\frac{L_{k-2}^{(n)}}{L_{k-1}^{(n)}}} \right), \tag{24}$$

where  $\delta_\omega < 1$  is predefined, and  $\hat{\omega}_{k-1} = \frac{t_{k-1}-1}{t_k}$  with  $t_0 = 1$ ,  $t_k = \frac{1}{2} \left( 1 + \sqrt{1 + 4t_{k-1}^2} \right)$ .

Let

$$\hat{\mathbf{A}}_{k-1}^{(n)} = \mathbf{A}_{k-1}^{(n)} + \omega_{k-1}^{(n)} \left( \mathbf{A}_{k-1}^{(n)} - \mathbf{A}_{k-2}^{(n)} \right) \tag{25}$$

denote an extrapolated point where  $\omega_{k-1}^{(n)}$  is the extrapolation weight, and let

$$\begin{aligned} \hat{\mathbf{G}}_{k-1}^{(n)} &= \hat{\mathbf{A}}_{k-1}^{(n)} \left[ \left( \mathbf{B}_{k-1}^{(n)} \right)^T \mathbf{B}_{k-1}^{(n)} + \alpha_n \mathbf{I}_R \right] \\ &\quad - \mathbf{X}_{(n)} \mathbf{B}^{(n)} + \beta_n \mathbf{E} \end{aligned} \tag{26}$$

represent the block-partial gradient of  $\mathcal{F}(\mathbf{A}^{(n)})$  at  $\hat{\mathbf{A}}_{k-1}^{(n)}$ . Factor  $\mathbf{A}^{(n)}$  at iteration  $k$  is updated by

$$\begin{aligned} \mathbf{A}_k^{(n)} &= \operatorname{argmin}_{\mathbf{A}^{(n)} \geq 0} \left\langle \hat{\mathbf{G}}_{k-1}^{(n)}, \mathbf{A}^{(n)} - \hat{\mathbf{A}}_{k-1}^{(n)} \right\rangle \\ &\quad + \frac{L_{k-1}^{(n)}}{2} \left\| \mathbf{A}^{(n)} - \hat{\mathbf{A}}_{k-1}^{(n)} \right\|_F^2. \end{aligned} \tag{27}$$

The closed form of (27) can be written as

$$\begin{aligned} \mathbf{A}_k^{(n)} &= \max \left( 0, \hat{\mathbf{A}}_{k-1}^{(n)} - \frac{\hat{\mathbf{G}}_{k-1}^{(n)}}{L_{k-1}^{(n)}} \right) \\ &= \max \left( 0, \hat{\mathbf{A}}_{k-1}^{(n)} - \frac{\hat{\mathbf{A}}_{k-1}^{(n)} \left[ \left( \mathbf{B}_{k-1}^{(n)} \right)^T \mathbf{B}_{k-1}^{(n)} + \alpha_n \mathbf{I}_R \right]}{L_{k-1}^{(n)}} \right. \\ &\quad \left. + \frac{\mathbf{X}_{(n)} \mathbf{B}^{(n)} - \beta_n \mathbf{E}}{L_{k-1}^{(n)}} \right). \end{aligned} \tag{28}$$

APG method for sparse NCP can be implemented by procedures in **Algorithm 4**.

### E. Alternating Nonnegative Least Squares

Alternating Nonnegative Least Squares (ANLS) is an important and efficient method for NMF problems [22], [25], [26]. Kim, H. and Kim, J. utilized ANLS to solve NMF with squared Frobenius-norm regularization and squared  $l_1$ -norm

---

**Algorithm 4:** APG for sparse NCP in (4)
 

---

**Input :**  $\mathcal{X}, R, \alpha, \beta, \delta_\omega$   
**Output:**  $\mathbf{A}^{(n)}, n = 1, \dots, N$   
 1 Initialize  $\mathbf{A}^{(n)} \in \mathbb{R}^{I_n \times R}, n = 1, \dots, N$ , using random numbers;  
 2 **for**  $k = 1, 2, \dots$  **do**  
 3     **for**  $n = 1$  **to**  $N$  **do**  
 4         Make mode- $n$  unfolding of  $\mathcal{X}$  as  $\mathbf{X}_{(n)}$ ;  
 5         Compute MTTKRP  $\mathbf{X}_{(n)}\mathbf{B}^{(n)}$  and  $(\mathbf{B}^{(n)})^T\mathbf{B}^{(n)}$  based on (8);  
 6         Compute  $L_{k-1}^{(n)}, \omega_{k-1}^{(n)}, \hat{\mathbf{A}}_{k-1}^{(n)}, \hat{\mathbf{G}}_{k-1}^{(n)}$  according to (23), (24), (25), (26);  
 7         Update  $\mathbf{A}_k^{(n)}$  according to (28);  
 8     **end**  
 9     **if**  $\vartheta(\mathbf{A}_k^{(n)}) > \vartheta(\mathbf{A}_{k-1}^{(n)})$  **then**  
 10          $\hat{\mathbf{A}}_{k-1}^{(n)} = \mathbf{A}_{k-1}^{(n)}$ , for  $n = 1, \dots, N$ ;  
 11         Update  $\mathbf{A}_k^{(n)}$  again according to (28);  
 12     **end**  
 13     **if** some termination criterion is reached **then**  
 14         **return**  $\mathbf{A}_k^{(n)}$ , for  $n = 1, \dots, N$ ;  
 15     **end**  
 16 **end**

---

sparse regularization [25], [26]. This idea can be naturally extended to the following sparsity regularized NCP problem:

$$\begin{aligned}
 \min_{\mathbf{A}^{(1)}, \dots, \mathbf{A}^{(N)}} \mathcal{O}_{\text{ANLS}} &= \frac{1}{2} \left\| \mathcal{X} - \llbracket \mathbf{A}^{(1)}, \dots, \mathbf{A}^{(N)} \rrbracket \right\|_F^2 \\
 &+ \sum_{n=1}^N \frac{\alpha_n}{2} \left\| \mathbf{A}^{(n)} \right\|_F^2 + \sum_{n=1}^N \frac{\beta_n}{2} \sum_{r=i}^{I_n} \left\| \left[ \mathbf{A}^{(n)} \right]_{(i,:)} \right\|_1^2 \\
 \text{s.t. } \mathbf{A}^{(n)} &\geq 0 \text{ for } n = 1, \dots, N,
 \end{aligned} \quad (29)$$

where  $\left[ \mathbf{A}^{(n)} \right]_{(i,:)}$  denotes the  $i$ th row of  $\mathbf{A}^{(n)}$ . Factors  $\mathbf{A}^{(n)}$  can be updated alternatively by the following minimization subproblem:

$$\begin{aligned}
 \min_{\mathbf{A}^{(n)}} \mathcal{F}_{\text{NNLS}} \left( \mathbf{A}^{(n)} \right) &= \frac{1}{2} \left\| \mathbf{X}_{(n)} - \mathbf{A}^{(n)} \left( \mathbf{B}^{(n)} \right)^T \right\|_F^2 \\
 &+ \frac{\alpha_n}{2} \left\| \mathbf{A}^{(n)} \right\|_F^2 + \frac{\beta_n}{2} \sum_{r=i}^{I_n} \left\| \left[ \mathbf{A}^{(n)} \right]_{(i,:)} \right\|_1^2 \\
 \text{s.t. } \mathbf{A}^{(n)} &\geq 0.
 \end{aligned} \quad (30)$$

By some simple mathematical operations, (30) is equivalent to the following minimization problem:

$$\begin{aligned}
 \min_{\mathbf{A}^{(n)}} \mathcal{F}_{\text{NNLS}} \left( \mathbf{A}^{(n)} \right) &= \\
 \frac{1}{2} \left\| \begin{pmatrix} \mathbf{B}^{(n)} \\ \sqrt{\alpha_n} \mathbf{I}_R \\ \sqrt{\beta_n} \mathbf{1}_{1 \times R} \end{pmatrix} \left( \mathbf{A}^{(n)} \right)^T - \begin{pmatrix} \mathbf{X}_{(n)}^T \\ \mathbf{0}_{R \times I_n} \\ \mathbf{0}_{1 \times I_n} \end{pmatrix} \right\|_F^2 \\
 \text{s.t. } \mathbf{A}^{(n)} &\geq 0,
 \end{aligned} \quad (31)$$

Afterwards, the partial derivative of  $\mathcal{F}_{\text{NNLS}} \left( \mathbf{A}^{(n)} \right)$  to  $\mathbf{A}^{(n)}$  is

$$\begin{aligned}
 \frac{\partial}{\partial \mathbf{A}^{(n)}} \mathcal{F}_{\text{NNLS}} \left( \mathbf{A}^{(n)} \right) \\
 = \mathbf{A}^{(n)} \left[ \left( \mathbf{B}^{(n)} \right)^T \mathbf{B}^{(n)} + \alpha_n \mathbf{I}_R + \beta_n \mathbf{E} \right] - \mathbf{X}_{(n)} \mathbf{B}^{(n)}.
 \end{aligned} \quad (32)$$

From (31) and (32), it is clear to see that the subproblem in (30) still satisfies the basic nonnegative least squares (NNLS) structure, which can be solve conveniently by those optimization methods for NNLS, such as active-set (AS) [25] and block principal pivoting (BPP) [26].

In (29), the squared  $l_1$ -norm of the rows in  $\mathbf{A}^{(n)}$  is used to impose sparsity in order to satisfy the NNLS structure, which is different from the sparse NCP in (4). **Algorithm 5** explicates the ANLS method for sparsity regularized NCP in (29).

---

**Algorithm 5:** ANLS for sparsity regularized NCP in (29)
 

---

**Input :**  $\mathcal{X}, R, \alpha, \beta$   
**Output:**  $\mathbf{A}^{(n)}, n = 1, \dots, N$   
 1 Initialize  $\mathbf{A}^{(n)} \in \mathbb{R}^{I_n \times R}, n = 1, \dots, N$ , using random numbers;  
 2 **repeat**  
 3     **for**  $n = 1$  **to**  $N$  **do**  
 4         Make mode- $n$  unfolding of  $\mathcal{X}$  as  $\mathbf{X}_{(n)}$ ;  
 5         Compute MTTKRP  $\mathbf{X}_{(n)}\mathbf{B}^{(n)}$  and  $(\mathbf{B}^{(n)})^T\mathbf{B}^{(n)}$  based on (8);  
 6          $(\mathbf{B}^{(n)})^T\mathbf{B}^{(n)} \leftarrow (\mathbf{B}^{(n)})^T\mathbf{B}^{(n)} + \alpha_n \mathbf{I}_R + \beta_n \mathbf{E}$ ;  
 7         Update factor  $\mathbf{A}^{(n)}$  using NNLS method based on (31);  
 8          $\mathbf{A}^{(n)} = \underset{\mathbf{A}^{(n)} \geq 0}{\operatorname{argmin}} \mathcal{F}_{\text{NNLS}} \left( \mathbf{A}^{(n)} \right)$   
 9         = NNLS\_AS  $(\mathbf{X}_{(n)}\mathbf{B}^{(n)}, (\mathbf{B}^{(n)})^T\mathbf{B}^{(n)})$   
 10         or  
 11         = NNLS\_BPP  $(\mathbf{X}_{(n)}\mathbf{B}^{(n)}, (\mathbf{B}^{(n)})^T\mathbf{B}^{(n)})$ .  
 12     **end**  
 13 **until** some termination criterion is reached;

---

#### IV. STOPPING CONDITION AND ACCELERATING STRATEGY

The optimization procedures for tensor decomposition are implemented by iterations. For NCP, a sequence of  $\left\{ \mathbf{A}_k^{(1)}, \dots, \mathbf{A}_k^{(N)} \right\}_{k=1}^\infty$  is produced at each iteration. It is necessary to terminate the iteration until some stopping condition is satisfied. Common stopping conditions includes the following: predefined maximum number of iterations, predefined maximum running time, the change of objective function value, the change of relative error (data fitting) [13], [45].

##### A. Objective Function and Relative Error

The computations of objective function value and relative error (data fitting) are highly correlated. In the  $k$ th iteration, the objective function value of NCP problem (2) is

$$\mathcal{O}_{\text{NCP}k} = \frac{1}{2} \left\| \mathcal{X} - \llbracket \mathbf{A}_k^{(1)}, \dots, \mathbf{A}_k^{(N)} \rrbracket \right\|_F^2, \quad (33)$$

and the relative error [13] is defined by

$$\text{RelErr}_k = \frac{\|\mathcal{X} - \llbracket \mathbf{A}_k^{(1)}, \dots, \mathbf{A}_k^{(N)} \rrbracket\|_F}{\|\mathcal{X}\|_F}. \quad (34)$$

Comparing (33) and (34), the relative error can also be computed from the objective function value directly:

$$\text{RelErr}_k = \frac{\sqrt{2\mathcal{O}_{\text{NCP}k}}}{\|\mathcal{X}\|_F}. \quad (35)$$

Meanwhile, the data fitting can be computed by

$$\text{Fit}_k = 1 - \text{RelErr}_k. \quad (36)$$

Based on the objective function value and the relative error, the stopping condition can be set by

$$|\text{RelErr}_{k-1} - \text{RelErr}_k| < \epsilon \quad (37)$$

or

$$|\mathcal{O}_{\text{NCP}k-1} - \mathcal{O}_{\text{NCP}k}| < \epsilon. \quad (38)$$

The threshold of  $\epsilon$  can be set by a very small positive value, such as  $1e-8$ .

### B. Accelerated Computation of Objective Function

By mode- $n$  unfolding of tensor, the objective function of NCP in (33) at the  $k$ th iteration can be represented equivalently as the following:

$$\mathcal{O}_{\text{NCP}k} = \frac{1}{2} \left\| \mathbf{X}_{(n)} - \mathbf{A}_k^{(n)} \left( \mathbf{B}_k^{(n)} \right)^T \right\|_F^2. \quad (39)$$

The works of [19] and [13] introduced a convenient idea to compute the objective function base on the trace computation of matrix. Inspired by this idea, we further represent the objective function in (39) by

$$\begin{aligned} & \mathcal{O}_{\text{NCP}k} \\ &= \frac{1}{2} \text{tr} \left\{ \left[ \mathbf{X}_{(n)} - \mathbf{A}_k^{(n)} \left( \mathbf{B}_k^{(n)} \right)^T \right]^T \left[ \mathbf{X}_{(n)} - \mathbf{A}_k^{(n)} \left( \mathbf{B}_k^{(n)} \right)^T \right] \right\} \\ &= \frac{1}{2} \left\{ \|\mathcal{X}\|_F^2 - 2 \text{tr} \left[ \mathbf{A}_k^{(n)} \left( \mathbf{X}_{(n)} \mathbf{B}_k^{(n)} \right)^T \right] \right. \\ & \quad \left. + \text{tr} \left[ \left( \mathbf{A}_k^{(n)} \right)^T \mathbf{A}_k^{(n)} \right] \left[ \left( \mathbf{B}_k^{(n)} \right)^T \mathbf{B}_k^{(n)} \right] \right\}. \end{aligned} \quad (40)$$

Furthermore, the objective function equals to

$$\mathcal{O}_{\text{NCP}k} = \frac{1}{2} \left\{ \|\mathcal{X}\|_F^2 - 2 \sum_{j=1}^R \sum_{i=1}^{I_n} \widehat{\mathbf{N}}_{i,j} + \sum_{j=1}^R \sum_{i=1}^R \widehat{\mathbf{M}}_{i,j} \right\}, \quad (41)$$

where  $\widehat{\mathbf{N}} = \mathbf{A}_k^{(n)} * \left( \mathbf{X}_{(n)} \mathbf{B}_k^{(n)} \right) \in \mathbb{R}^{I_n \times R}$  and  $\widehat{\mathbf{M}} = \left( \left( \mathbf{A}_k^{(n)} \right)^T \mathbf{A}_k^{(n)} \right) * \left( \left( \mathbf{B}_k^{(n)} \right)^T \mathbf{B}_k^{(n)} \right) \in \mathbb{R}^{R \times R}$ . Here,  $*$  is the Hadamard product.

Since tensor data usually consist of a large amount of data points, the computation of the objective function at each iteration will be time consuming by (33) or (39). For example, in (39) the computational complexity of  $\mathbf{A}_k^{(n)} \left( \mathbf{B}_k^{(n)} \right)^T$  is

$O(R \times \prod_{n=1}^N I_n)$ . On the other hand, by observing **Algorithm 1 to 5**, we find that the items of  $\mathbf{X}_{(n)} \mathbf{B}_k^{(n)}$  and  $\left( \mathbf{B}_k^{(n)} \right)^T \mathbf{B}_k^{(n)}$  have been computed in advance in order to update  $\mathbf{A}_k^{(n)}$ . Therefore, these two items can be employed directly to compute the objective function by (41). In (41), the computational complexity of  $\widehat{\mathbf{N}}$  and  $\widehat{\mathbf{M}}$  is only  $O(I_n R + R^2)$ , which has been reduced significantly.

### C. Computation of Objective Function for Sparse NCP

The objective function and relative error for sparse NCP should be carefully considered, due to the extra Frobenius norm and  $l_1$ -norm regularization items. Based on the relationship introduced in Subsection IV-A and the accelerating method in Subsection IV-B, the computation of objective function and relative error for sparse NCP is explicated in **Algorithm 6**.

---

**Algorithm 6:** Objective function and relative error for sparse NCP

---

**Input :**  $\mathcal{X}$ ,  $R$ ,  $\alpha$ ,  $\beta$ ,  $\epsilon$

**Output:**  $\mathbf{A}^{(n)}$ ,  $n = 1, \dots, N$

```

1 Initialize  $\mathbf{A}^{(n)} \in \mathbb{R}^{I_n \times R}$ ,  $n = 1, \dots, N$ , using random
  numbers;
2 repeat
3   (Supposing this is the  $k$ th iteration)
4   for  $n = 1$  to  $N$  do
5     Make mode- $n$  unfolding of  $\mathcal{X}$  as  $\mathbf{X}_{(n)}$ ;
6     Compute MTTKRP  $\mathbf{X}_{(n)} \mathbf{B}_k^{(n)}$  and  $\left( \mathbf{B}_k^{(n)} \right)^T \mathbf{B}_k^{(n)}$ 
      based on (8);
7     Update factor  $\mathbf{A}_k^{(n)}$  using optimization method;
8   end
9   Compute  $\mathcal{O}_{\text{NCP}k}$  using (41), in which  $n = N$ ;
10  Compute  $\text{RelErr}_k$  using (35);
11  Let the objective function of sparse NCP
      $\mathcal{O}_k = \mathcal{O}_{\text{NCP}k}$ ;
12  for  $n = 1$  to  $N$  do
13     $\mathcal{O}_k = \mathcal{O}_k + \frac{\alpha_n}{2} \left\| \mathbf{A}_k^{(n)} \right\|_F^2 + \beta_n \sum_{r=1}^R \left\| \mathbf{a}_{rk}^{(n)} \right\|_1$ ;
14  end
15  if  $|\mathcal{O}_{k-1} - \mathcal{O}_k| < \epsilon$  then
16    | Terminate iterating.
17  end
18  or
19  if  $|\text{RelErr}_{k-1} - \text{RelErr}_k| < \epsilon$  then
20    | Terminate iterating.
21  end
22 until some termination criterion is reached;
    
```

---

For ANLS method, the **step 13** in **Algorithm 6** should be changed into

$$\mathcal{O}_k = \mathcal{O}_k + \frac{\alpha_n}{2} \left\| \mathbf{A}_k^{(n)} \right\|_F^2 + \frac{\beta_n}{2} \sum_{r=i}^{I_n} \left\| \left[ \mathbf{A}_k^{(n)} \right]_{(i,:)} \right\|_1^2$$

according to (29).

## V. EXPERIMENTS AND RESULTS

We carried out the experiments on synthetic tensor data and real tensor data, both of which contain third-order and fourth-order cases. We compared the abilities of sparse NCP methods to impose sparsity implemented by MU, ALS, HALS, APG, ANLS-AS and ANLS-BPP.

In all sparse NCP experiments, the factor matrices were initialized using nonnegative normally distributed random numbers by MATLAB function  $\max(0, \text{randn}(I_n, R))$ . We keep the Frobenius norm regularization in the sparse NCP model to make a fair comparison for all methods, especially the comparison of the objective function, although it is not necessary for some optimization methods, such as ANLS-AS, APG, HALS and MU. We set the Frobenius norm parameters by  $\alpha_1 = \alpha_2 = \dots = \alpha_N = 1e - 6$ . The  $l_1$ -norm regularization parameters of  $\beta_n, n = 1, \dots, N$ , in sparse NCP are the key elements to impose sparsity, which are the most important testing parameters in the experiments. In order to make it convenient to select and test the parameters, we also kept  $\beta_n, n = 1, \dots, N$ , the same in all modes of the tensor. After selecting the  $\beta_n$ , we calculated and evaluated the sparsity level [35] of the factor matrices by

$$\text{Sparsity}_{\mathbf{A}^{(n)}} = \frac{\#\left\{\mathbf{A}_{i,r}^{(n)} < T_s\right\}}{I_n \times R}, \quad (42)$$

where  $\#\{\cdot\}$  denotes the number of elements that are smaller than the threshold  $T_s$  in factor matrix  $\mathbf{A}^{(n)}$ . In the experiments, we selected  $T_s = 1e - 3$ .

All the experiments were conducted on computer with Intel Core i5-4590 3.30GHz CPU, 8GB memory, 64-bit Windows 10 and MATLAB R2016b. The fundamental tensor computation was based on Tensor Toolbox 2.6 [46]–[48].

### A. Third-Order Synthetic Data

In the first experiment, we constructed a synthetic third-order tensor by 10 channels of simulated sparse and nonnegative signals<sup>1</sup>, as shown in Fig. 1(a). There are 1000 points in each channel, so the signal matrix is  $\mathbf{S}^{(1)} = [\mathbf{s}_1, \dots, \mathbf{s}_{10}] \in \mathbb{R}^{1000 \times 10}$ . Two uniformly distributed random matrices  $\mathbf{A}^{(2)}, \mathbf{A}^{(3)} \in \mathbb{R}^{100 \times 10}$  were employed as mixing matrices, which were generated by `rand` function in MATLAB. Afterwards, we synthesized the third-order tensor by  $\mathcal{X}_{\text{Syn-3rd}} = \llbracket \mathbf{S}^{(1)}, \mathbf{A}^{(2)}, \mathbf{A}^{(3)} \rrbracket \in \mathbb{R}^{1000 \times 100 \times 100}$ . Next, nonnegative Gaussian noise was added to the tensor with SNR of 40dB, which was generated by MATLAB code  $\max(0, \text{randn}(\text{size}(\mathcal{X})))$ .

For all sparse NCP methods, we used the stop condition of relative error change in (37), in which the threshold is  $\epsilon = 1e - 8$ . The maximum running time was set by 180 seconds. We selected a larger value of 20 as the number of components for tensor decomposition<sup>2</sup>. The reason is that

<sup>1</sup>The sparse signals come from the file of `vSparse_rand_10.mat` included in NMFLAB, which can be downloaded from <http://www.bsp.brain.riken.jp/ICALAB/nmflab.html>

<sup>2</sup>Since 10 channels of signals are mixed in the tensor, naturally, 10 should be selected as the optimal component number. The number of components might also be estimated by some classical methods, such as DIFFIT [49]. However, we selected 20 according to the purpose of the experiment.

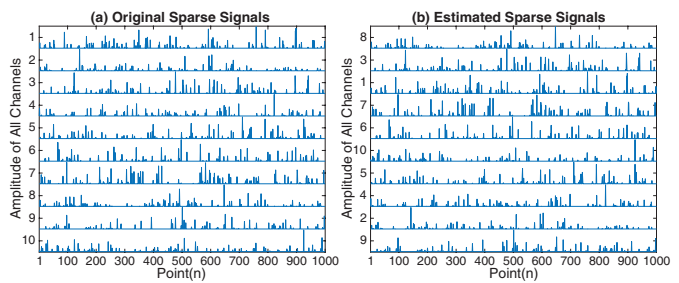


Fig. 1. Sparse and nonnegative signals used in synthetic tensor. (a) shows the original ten channels of signals. (b) shows the estimated ten channels of signals from third-order synthetic tensor by sparse NCP based on ANLS-BPP method, in which  $\beta_n = 0.5$ .

we intend to recover the 10 channels of true signal just by imposing sparse regularization during decomposition, even though we don't know the exact optimal number of components. We selected values of  $\beta_n = 0, 0.1, 0.5, 1, 2, 3$  for all the optimization methods to evaluate their abilities to impose sparsity. The selection of sparse regularization parameters depends on the tensor data. After tensor decomposition, the values of objective function value, relative error, running time, iteration number, the sparsity level and nonzero component number of the estimated signal factor matrix were recorded as the performance evaluation criteria. For all optimization methods with each  $\beta_n$ , the sparse NCP was run 30 times, and the average values of all criteria were computed. The results are shown in **Table I**.

From **Table I**, it can be found that all ANLS-AS, ANLS-BPP, APG, MU, ALS methods can impose sparsity with proper sparse regularization parameter  $\beta_n$ . With certain sparse regularization, 10 nonzero components are retained in the mode-1 factor matrix, which represent the 10 channels of sparse signals extracted from the mixed tensor. ANLS-AS, ANLS-BPP, APG, and ALS exhibit comparatively low relative errors and less running time, whereas MU converges very slowly. On the other hand, HALS fails to impose sparsity even with a larger  $\beta_n$  and can hardly reduce the number of nonzero components. HALS also has very large objective function value and high relative error with larger  $\beta_n$ .

It can be inferred from **Table I** that, after properly tuning the sparse regularization parameter  $\beta_n$ , weak components will be removed (set to 0), weak elements in strong components will be prohibited, and the true 10 channels of sparse signals will be recovered. One of the recovered sparse signal matrix by ANLS-BPP is shown in Fig. 1(b). Afterwards, the accuracy of the recovered signals should be evaluated. Let  $\mathbf{T}^{(1)} = [\mathbf{t}_1, \dots, \mathbf{t}_{\tilde{R}}] \in \mathbb{R}^{L \times \tilde{R}}$  represent the estimated matrix of sparse signals, in which  $\tilde{R}$  is the number of nonzero components and  $L$  is the length of component ( $L = 1000$  in this experiment). We evaluate the accuracy of the estimated matrix  $\mathbf{T}^{(1)}$  compared with original sparse signals  $\mathbf{S}^{(1)}$  by Peak Signal-to-Noise-Ratio (PSNR, see Chapter 3 in [1])

$$\text{PSNR} = \frac{1}{\tilde{R}} \sum_{r=1}^{\tilde{R}} 10 \log_{10} \left( \frac{L}{\left\| \hat{\mathbf{t}}_r - \hat{\mathbf{s}}_c \right\|_2^2} \right), \quad (43)$$



TABLE I  
COMPARISON OF SPARSE NCPs ON SYNTHETIC TENSOR DATA

Algorithm	$\beta_n$	Third-order Synthetic Tensor						Fourth-order Synthetic Tensor					
		Obj	RelErr	Time	Iter	Sparsity	Comp	Obj	RelErr	Time	Iter	Sparsity	Comp
ANLS AS	0	9.7243e+01	0.0082	8.6	168.1	0.6087	19.87	1.5094e+02	0.0082	87.8	43.7	0.6835	19.20
	0.1	7.3466e+02	0.0083	14.1	357.3	<b>0.9096</b>	<b>10.00</b>	9.5641e+02	0.0084	92.0	45.6	<b>0.8506</b>	<b>10.07</b>
	0.5	2.1466e+03	0.0084	67.1	1713.7	0.7222	<b>10.00</b>	3.2866e+03	0.0085	412.2	204.8	<b>0.8700</b>	<b>10.00</b>
	1	4.1733e+03	0.0084	50.0	1274.1	0.7198	<b>10.00</b>	4.3322e+03	0.0085	1043.8	520.2	<b>0.8879</b>	<b>10.00</b>
	2	8.2378e+03	0.0087	29.8	751.3	0.7211	<b>10.00</b>	6.4106e+03	0.0086	1283.3	641.8	<b>0.8896</b>	<b>10.00</b>
	3	1.2298e+04	0.0092	21.7	546.0	0.7235	<b>10.00</b>	8.3929e+03	0.0087	1547.8	768.0	<b>0.8673</b>	<b>10.00</b>
ANLS BPP	0	9.7240e+01	0.0082	8.2	165.6	0.6173	19.90	1.5095e+02	0.0082	99.5	49.8	0.6848	19.23
	0.1	7.3447e+02	0.0083	16.4	390.0	<b>0.9045</b>	<b>10.00</b>	9.1615e+02	0.0085	82.3	41.0	<b>0.8658</b>	<b>10.23</b>
	0.5	2.1475e+03	0.0084	70.8	1735.1	0.7228	<b>10.00</b>	3.2693e+03	0.0085	362.1	181.0	<b>0.8679</b>	<b>10.00</b>
	1	4.1734e+03	0.0084	52.0	1269.6	0.7195	<b>10.00</b>	4.4226e+03	0.0085	1116.8	559.7	<b>0.8716</b>	<b>10.00</b>
	2	8.2374e+03	0.0087	31.5	762.4	0.7213	<b>10.00</b>	6.5015e+03	0.0086	1192.1	596.8	<b>0.8886</b>	<b>10.00</b>
	3	1.2298e+04	0.0092	22.4	540.3	0.7237	<b>10.00</b>	8.3143e+03	0.0087	1594.6	795.6	<b>0.8704</b>	<b>10.00</b>
APG	0	9.7435e+01	0.0082	37.5	992.0	0.4195	20.00	1.5378e+02	0.0083	1292.9	647.1	0.1841	20.00
	0.1	5.0500e+02	0.0083	12.0	321.6	0.5187	19.83	6.9398e+02	0.0085	448.6	224.8	0.5522	15.50
	0.5	1.7657e+03	0.0084	12.5	334.3	0.6363	17.83	2.4718e+03	0.0085	421.3	211.1	0.6549	12.70
	1	2.9607e+03	0.0084	25.5	667.3	0.7365	14.97	4.4068e+03	0.0086	500.7	249.7	0.7092	12.13
	2	4.2958e+03	0.0084	68.2	1824.5	<b>0.8980</b>	<b>10.67</b>	6.4829e+03	0.0087	969.8	486.4	<b>0.7863</b>	<b>10.97</b>
	3	6.2480e+03	0.0085	60.9	1632.1	<b>0.9086</b>	<b>10.73</b>	8.1431e+03	0.0088	1106.6	557.3	<b>0.8270</b>	<b>10.67</b>
MU	0	9.8720e+01	0.0083	180	4976.2	0.7270	20.00	1.6924e+02	0.0087	1800	902.2	0.7072	20.00
	0.1	3.5118e+02	0.0084	158.4	4364.9	0.8435	17.07	4.6624e+02	0.0087	1800	898.4	0.7709	19.77
	0.5	1.1763e+03	0.0084	134.5	3704.6	0.8726	13.00	1.4612e+03	0.0087	1800	897.4	0.8410	16.30
	1	2.1223e+03	0.0084	131.7	3625.6	0.8728	11.33	2.5216e+03	0.0087	1800	904.3	0.8722	14.57
	2	3.9818e+03	0.0084	134.7	3720.2	0.8720	<b>10.50</b>	4.2640e+03	0.0087	1800	897.8	0.8973	12.80
	3	5.9273e+03	0.0085	123.8	3416.9	0.8640	<b>10.43</b>	5.9319e+03	0.0088	1800	898.6	0.9022	12.20
HALS	0	9.8608e+01	0.0082	25.7	670.6	0.8453	20.00	1.5537e+02	0.0083	491.6	244.6	0.8636	20.00
	0.1	4.1446e+03	0.0099	10.6	274.7	0.7929	20.00	1.3866e+03	0.0084	442.5	220.1	0.8331	20.00
	0.5	1.9432e+04	0.0222	17.7	460.1	0.6651	20.00	6.2725e+03	0.0089	678.6	339.8	0.7907	19.53
	1	3.7638e+04	0.0364	16.0	413.3	0.6034	20.00	1.2357e+04	0.0102	367.1	183.4	0.7512	19.57
	2	7.2050e+04	0.0603	13.0	338.3	0.5462	19.93	2.4423e+04	0.0141	223.1	111.3	0.7180	19.33
	3	1.0444e+05	0.0812	14.0	362.8	0.5130	19.97	3.6296e+04	0.0184	227.8	113.0	0.7168	19.10
ALS	0	1.0115e+02	0.0083	9.2	234.5	0.6350	16.73	1.6167e+02	0.0083	152.7	76.1	0.6418	17.00
	0.1	5.5442e+02	0.0085	14.7	405.0	<b>0.9278</b>	<b>10.20</b>	5.6488e+03	0.0163	657.5	327.4	<b>0.7884</b>	<b>10.30</b>
	0.5	1.5598e+03	0.0083	44.9	1228.3	<b>0.9157</b>	<b>10.03</b>	1.0572e+04	0.0164	926.7	467.1	<b>0.8084</b>	<b>10.10</b>
	1	2.2705e+03	0.0084	88.9	2416.1	<b>0.8938</b>	<b>10.00</b>	1.1493e+04	0.0171	1244.0	621.5	<b>0.8050</b>	<b>9.93</b>
	2	4.5176e+03	0.0085	90.0	2463.6	<b>0.8896</b>	<b>10.00</b>	1.8490e+04	0.0241	1160.1	579.9	<b>0.8090</b>	<b>9.90</b>
	3	6.6982e+03	0.0085	79.4	2177.8	<b>0.8810</b>	<b>10.00</b>	2.2452e+04	0.0256	1187.6	593.5	<b>0.8472</b>	<b>9.87</b>

**Note:** For the third-order synthetic tensor, the threshold of stopping condition is 1e-8 based on relative error change, and the maximum running time is 180s. For the fourth-order synthetic tensor, the threshold is 1e-7, and the maximum running time is 1800s. The values are the average after 30 times of running.

where  $\hat{t}_r$  is the  $r$ th normalized estimated sparse signal, and  $\hat{s}_c$  is the normalized reference sparse signal.  $\hat{s}_c$  comes from  $\mathbf{S}^{(1)}$ , which has the highest correlation coefficient with  $\hat{t}_r$ . For all the optimization methods with each  $\beta_n$ , all the PSNR values were recorded after 30 times of running of sparse NCP. Subsequently, box plot of PSNR for MU, ALS, HALS, APG, ANLS-AS, ANLS-BPP was drawn in Fig. 2.

In Fig. 2, it is clear that APG and ALS methods have higher PSNR at larger sparse regularization parameters of  $\beta_n = 2, 3$ , with which they recover the 10 channels of sparse signals more precisely. For ANLS-AS and ANLS-BPP, their PSNR values decrease when  $\beta_n > 0.5$ . The reason might be that ANLS framework uses the squared  $l_1$ -norm as the sparse regularization item, which is more sensitive to the sparse regularization parameter  $\beta_n$  (smaller  $\beta_n$  will cause higher

sparsity, and larger  $\beta_n$  might spoil the decomposition). Fig. 2 also shows that HALS performs poorly with sparse regularization.

We also recorded the objective function values of all sparse NCP methods within the first 30 seconds. The results of these methods with  $\beta_n = 0, 0.1, 1, 2$  are shown in Fig. 3. In the results, we find that MU converges very slowly in all cases, but it can minimize the objective function to a low level gradually. ALS method is not stable, which sometimes can't ensure that the objective function decreases. However, the stability of ALS will be improved with higher sparse regularization parameters. HALS runs much fast, but its objective function becomes very large when sparse regularization is added. APG shows excellent performances in both running speed and the ability to minimize the objective function in the third-order tensor

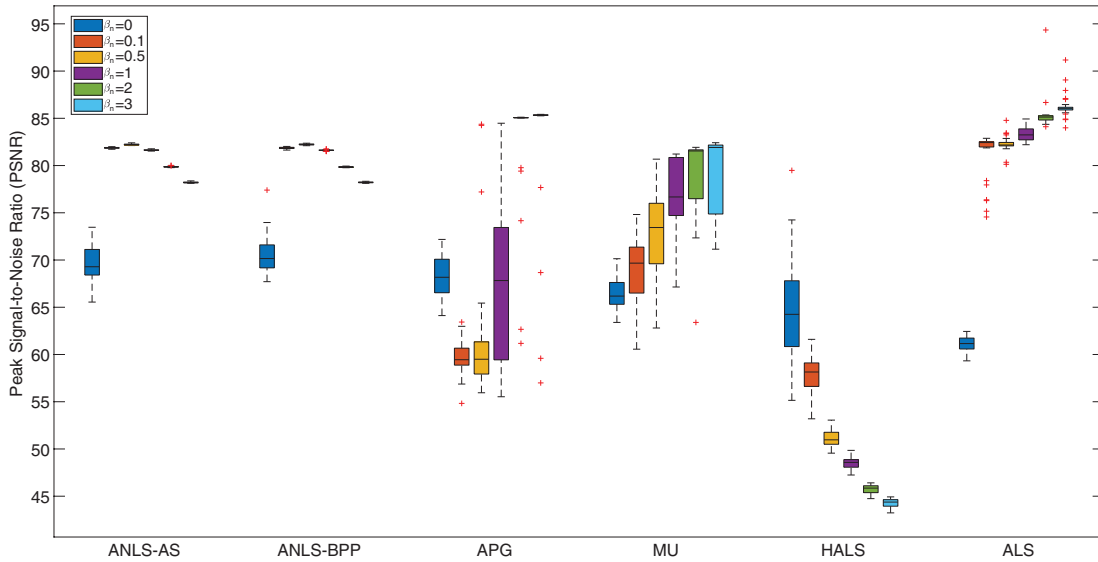


Fig. 2. Boxplot of Peak Signal-to-Noise Ratio (PSNR) for sparse NCP methods on third-order synthetic tensor. The PSNR is a measure of accuracy of the estimated sparse signals compared with the true signals.

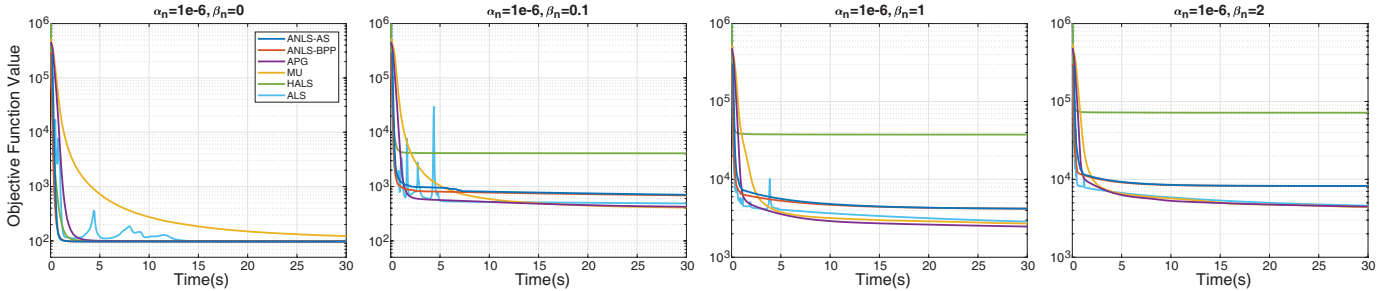


Fig. 3. The Objective Function Value Curves of Sparse NCPs on Third-order Synthetic Tensor With Fixed Time Limit of 30s.

case. ANLS-AS and ANLS-BPP can minimize the objective function very fast at the beginning, but their objective function values are a bit higher when sparse regularization is added. This is due to the squared  $l_1$ -norm item in ANLS framework.

**B. Fourth-Order Synthetic Data**

In the second experiment, we synthesized a fourth-order tensor by the same 10 channels of simulated sparse and nonnegative signals as that in last section. The tensor was synthesized by  $\mathcal{X}_{\text{Syn-4th}} = \llbracket \mathbf{S}^{(1)}, \mathbf{A}^{(2)}, \mathbf{A}^{(3)}, \mathbf{A}^{(4)} \rrbracket \in \mathbb{R}^{1000 \times 100 \times 100 \times 5}$ , in which  $\mathbf{S}^{(1)}$  is the simulated sparse signals, and  $\mathbf{A}^{(2)}, \mathbf{A}^{(3)} \in \mathbb{R}^{100 \times 10}, \mathbf{A}^{(4)} \in \mathbb{R}^{5 \times 10}$  are random matrices in uniform distribution. Nonnegative Gaussian noise was added to this fourth-order tensor with SNR of 40dB.

Processing higher-order (order  $\geq 4$ ) is very challenging due to the huge amount of data and the high complexity of optimization method. In this fourth-order tensor experiment, we selected  $\epsilon = 1e-7$  as the threshold of stopping condition based on the relative error change in (37), and set 1800 seconds as the maximum running time. Other parameter settings and experimental methods are the same as those in subsection V-A. The averages of objective function, relative error, running time, iteration number, the sparsity level and nonzero component number of the estimated signal factor matrix after 30 times

of running are recorded in **Table I**. The box plot of PSNR for all methods after 30 times of run is shown in **Fig. 4**. The results of the fourth-order synthetic tensor decomposition in **Table I** and **Fig. 4** have proven once more the effectiveness of MU, ALS, APG, ANLS-AS, ANLS-BPP to impose sparsity and estimate the true sparse signals.

We recorded the objective function values of all sparse NCP methods for the fourth-order tensor within the first 600 seconds. The results of these methods with  $\beta_n = 0, 0.1, 1, 2$  are shown in **Fig. 5**. It is clear to see that ALS method is still not stable, which can't guarantee the objective function to decrease. MU method still shows slow convergence. Surprisingly, the APG method that presents excellent performance for third-order tensor runs very slowly for the fourth-order tensor, which performs even more poorly than MU at the first tens of seconds. HALS has very large objective function value when sparse regularization is imposed. However, both ANLS-AS and ANLS-BPP still converge very fast for the fourth-order sparse NCP. When sparse regularization is imposed, ANLS-AS and ANLS-BPP have slightly higher objective function values due to the squared  $l_1$ -norm item in ANLS framework.

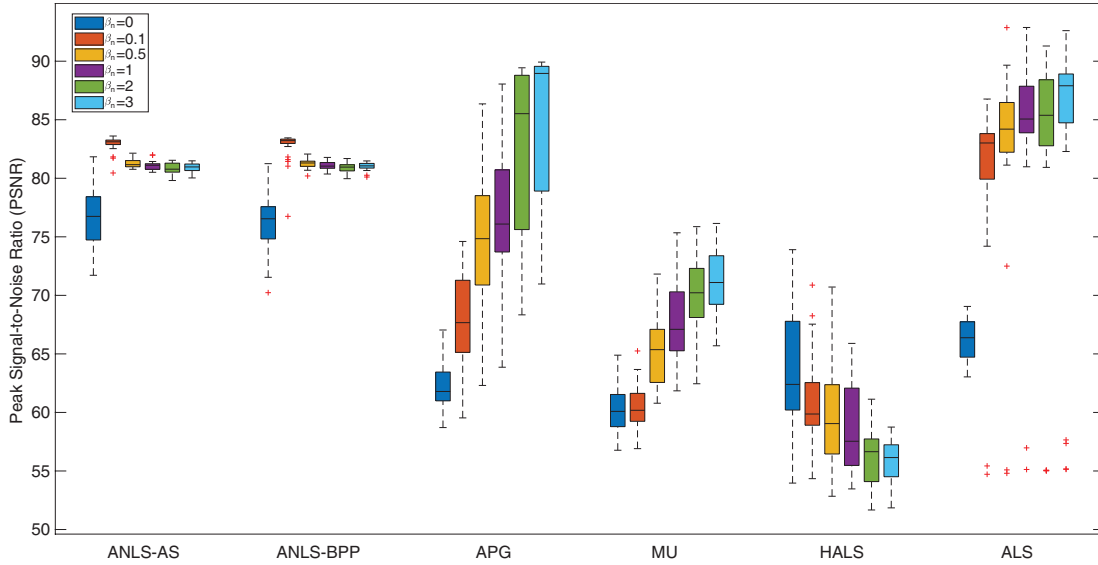


Fig. 4. Boxplot of Peak Signal-to-Noise Ratio (PSNR) for sparse NCP methods on Fourth-order synthetic tensor. The PSNR is a measure of accuracy of the estimated sparse signals compared with the true signals.

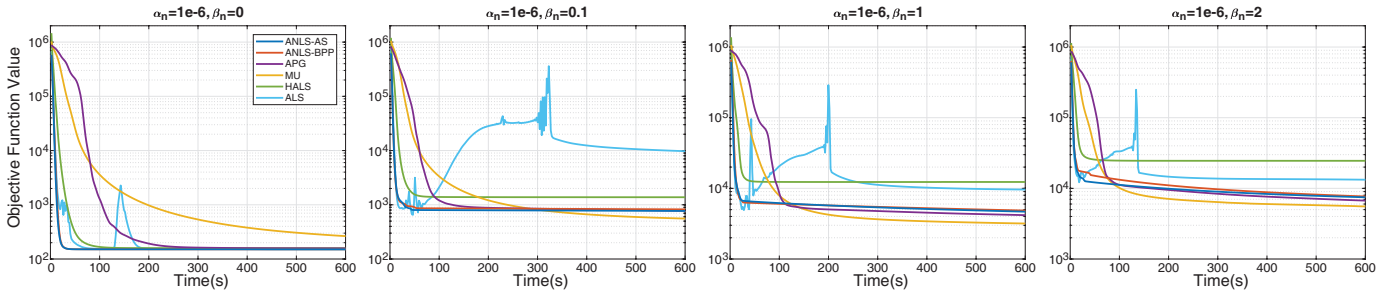


Fig. 5. The Objective Function Value Curves of Sparse NCPs on Fourth-order Synthetic Tensor With Fixed Time Limit of 600s.

### C. Third-Order ERP Data

In the third experiment, we utilized an open preprocessed ERP tensor<sup>3</sup>. Original data are organized in fourth-order form, whose size is channel  $\times$  frequency  $\times$  time  $\times$  subject-group =  $9 \times 71 \times 60 \times 42$ . The 9 channel points denote the 9 electrodes on the scalp, the 71 frequency points show the spectrum within 1-15Hz, the 60 time points illustrate the temporal energy between 0-300ms, and the 42 subject-group points include 21 subjects with reading disability (RD) and 21 subjects with attention deficit (AD) [50]. In this experiment, we merged the modes of frequency and time, by which the original tensor was reshaped into a third-order tensor with size channel  $\times$  frequency-time  $\times$  subject-group =  $9 \times 4260 \times 42$ .

For this third-order tensor, the number of components is set by 40 according to previous study [50]. For all methods, the threshold of stopping condition was set by  $1e-8$  based on the relative error change, and the maximum running time was 240s. The values of  $\beta_n = 0, 10, 50, 100, 200, 300$  were tested for all methods. We recorded the objective function, relative error, running time, iteration number, the sparsity level and nonzero component number of the frequency-time factor

matrix for all methods. The average values after 30 times of run are recorded in **Table II**.

It can be found from **Table II** that ANLS-AS, ANLS-BPP and APG are very effective to impose sparsity on the factor matrix and reduce components number by adjusting  $\beta_n$ , which costs comparatively less time. MU is not very effective to impose sparsity, which often reaches the limit of running time with slow convergence. Both HALS and ALS fail to impose proper sparsity by adjusting  $\beta_n$ , which also show high objective function values and relative errors with large  $\beta_n$ .

We also recorded the objective function values of all methods within the first 120 seconds. The results of these methods with  $\beta_n = 0, 10, 50, 100$  are displayed in **Fig. 6**. **Fig. 6** shows that MU still converges very slowly and ALS is not stable. When sparse regularization is added, HALS has very large objective function value. ANLS-AS and ANLS-BPP converge fast at the beginning, but have slightly higher objective function values with  $\beta_n > 0$  due to the squared  $l_1$ -norm regularization item. APG has excellent performances in both speed and convergence for this third-order ERP tensor.

### D. Fourth-Order ERP Data

In the fourth experiment, we applied all the sparse NCP algorithms to the original fourth-order ERP tensor introduced

<sup>3</sup>Data website: [http://www.escience.cn/people/cong/AdvancedSP\\_ERP.html](http://www.escience.cn/people/cong/AdvancedSP_ERP.html)

TABLE II  
COMPARISON OF SPARSE NCPs ON ERP TENSOR DATA

Algorithm	$\beta_n$	Third-order ERP Tensor						Fourth-order ERP Tensor					
		Obj	RelErr	Time	Iter	Sparsity	Comp	Obj	RelErr	Time	Iter	Sparsity	Comp
ANLS AS	0	3.2211e+05	0.0916	119.5	1410.9	<b>0.2594</b>	38.87	5.8001e+05	0.1229	18.6	608.5	<b>0.3338</b>	34.17
	10	1.1203e+06	0.1439	44.3	687.9	<b>0.5645</b>	20.80	9.9992e+05	0.1360	20.2	686.8	<b>0.4283</b>	29.60
	50	2.2425e+06	0.1989	33.7	549.3	<b>0.7416</b>	11.53	1.8522e+06	0.1655	16.1	556.7	<b>0.5640</b>	21.77
	100	3.0417e+06	0.2376	25.3	413.7	<b>0.8200</b>	7.83	2.4220e+06	0.1891	13.5	491.2	<b>0.6521</b>	16.43
	200	3.8588e+06	0.2731	24.0	397.0	<b>0.8774</b>	5.27	3.1446e+06	0.2185	12.1	456.1	<b>0.7380</b>	11.90
	300	4.3772e+06	0.2963	17.7	290.3	<b>0.9071</b>	3.93	3.6604e+06	0.2346	11.9	438.5	<b>0.7715</b>	10.33
ANLS BPP	0	3.1067e+05	0.0900	119.7	1498.7	<b>0.2509</b>	39.70	5.6736e+05	0.1216	23.4	713.4	<b>0.3247</b>	34.90
	10	1.1248e+06	0.1451	40.9	691.9	<b>0.5740</b>	20.37	9.9176e+05	0.1346	20.0	694.1	<b>0.4230</b>	30.00
	50	2.2574e+06	0.2015	26.5	479.7	<b>0.7480</b>	11.17	1.8548e+06	0.1651	14.6	517.0	<b>0.5660</b>	21.77
	100	3.0346e+06	0.2350	26.5	480.7	<b>0.8146</b>	8.10	2.4312e+06	0.1899	13.2	469.8	<b>0.6560</b>	16.37
	200	3.8466e+06	0.2715	27.1	507.1	<b>0.8743</b>	5.47	3.1594e+06	0.2158	9.8	362.4	<b>0.7294</b>	12.23
	300	4.3186e+06	0.2914	21.7	406.0	<b>0.9020</b>	4.20	3.6794e+06	0.2350	13.3	480.5	<b>0.7690</b>	10.43
APG	0	3.0688e+05	0.0895	134.4	2540.1	<b>0.2602</b>	40.00	4.8108e+05	0.1120	99.1	2113.5	<b>0.2468</b>	40.00
	10	3.8277e+05	0.0897	119.9	2247.9	<b>0.2861</b>	40.00	6.6882e+05	0.1263	71.5	1525.3	<b>0.3509</b>	33.03
	50	6.6367e+05	0.0919	89.1	1678.9	<b>0.3160</b>	39.03	1.2169e+06	0.1651	36.2	775.0	<b>0.5748</b>	20.73
	100	1.0160e+06	0.1004	54.8	1038.4	<b>0.3783</b>	35.67	1.6803e+06	0.1936	30.1	655.7	<b>0.6793</b>	15.03
	200	1.6074e+06	0.1226	43.2	824.2	<b>0.5075</b>	27.33	2.5051e+06	0.2367	22.3	486.2	<b>0.7860</b>	9.60
	300	2.1091e+06	0.1447	37.0	708.7	<b>0.6003</b>	21.23	2.9254e+06	0.2555	20.2	437.8	<b>0.8217</b>	7.73
MU	0	3.3865e+05	0.0940	240	5165.7	0.2466	40.00	5.0307e+05	0.1145	120	4490.9	0.2408	40.00
	10	4.1809e+05	0.0950	240	4934.4	0.3004	40.00	5.4429e+05	0.1149	120	4478.4	0.2445	40.00
	50	6.9031e+05	0.0951	240	5070.4	0.3079	39.80	6.7206e+05	0.1147	120	4470.2	0.2502	40.00
	100	1.0382e+06	0.0991	240	5035.2	0.3374	38.77	8.3825e+05	0.1148	120	4706.8	0.2501	39.97
	200	1.6559e+06	0.1150	153.3	3090.9	0.4366	33.33	1.1797e+06	0.1170	119.2	4697.8	0.2637	39.53
	300	2.1959e+06	0.1296	73.0	1588.1	0.5004	29.27	1.5014e+06	0.1207	111.3	4351.7	0.2949	38.07
HALS	0	3.0571e+05	0.0893	139.8	2864.5	0.3287	40.00	4.8047e+05	0.1119	48.5	1780.7	0.2458	40.00
	10	1.1920e+06	0.1075	28.6	579.5	0.1869	40.00	1.4878e+06	0.1318	16.1	593.7	0.1784	40.00
	50	3.7030e+06	0.1479	29.3	592.4	0.0683	40.00	4.1396e+06	0.1779	15.1	555.7	0.0855	40.00
	100	6.3899e+06	0.1845	25.6	521.5	0.0409	40.00	6.8072e+06	0.2177	17.2	622.6	0.0377	40.00
	200	1.1155e+07	0.2471	91.1	1859.7	0.1135	35.93	1.1392e+07	0.2763	33.6	1219.8	0.0602	38.17
	300	1.5526e+07	0.3137	175.1	3510.1	0.2825	29.00	1.5458e+07	0.3332	10.1	371.8	0.1817	33.07
ALS	0	1.4336e+06	0.1822	237.6	4079.6	0.6615	20.97	1.6875e+06	0.1474	115.1	2266.5	0.5117	26.27
	10	5.4467e+06	0.1706	228.2	4219.0	0.7123	18.63	7.1430e+06	0.1619	119.0	2465.7	0.5151	27.07
	50	6.0430e+06	0.2058	140.6	2711.0	0.9208	5.53	7.3298e+06	0.1764	114.9	2507.3	0.5579	24.23
	100	8.4312e+06	0.3773	21.7	459.6	0.9454	2.83	7.7009e+06	0.1738	116.5	2955.9	0.5582	24.13
	200	2.3166e+07	0.7066	12.4	275.5	0.9817	0.87	7.0916e+06	0.1899	95.9	2605.2	0.6020	20.77
	300	3.5148e+07	0.9392	2.0	44.0	0.9968	0.13	7.4508e+06	0.1955	83.3	2445.7	0.6307	18.83

**Note:** The threshold of stopping condition is  $1e-8$  based on relative error change. For the third-order tensor, the maximum running time is 240s, and the sparsity and nonzero component number are computed based on the frequency-time factor matrix. For the fourth-order tensor, the maximum running time is 120s, and the sparsity and nonzero component number are computed based on the temporal factor matrix. The values in the table are the average after 30 times of running.

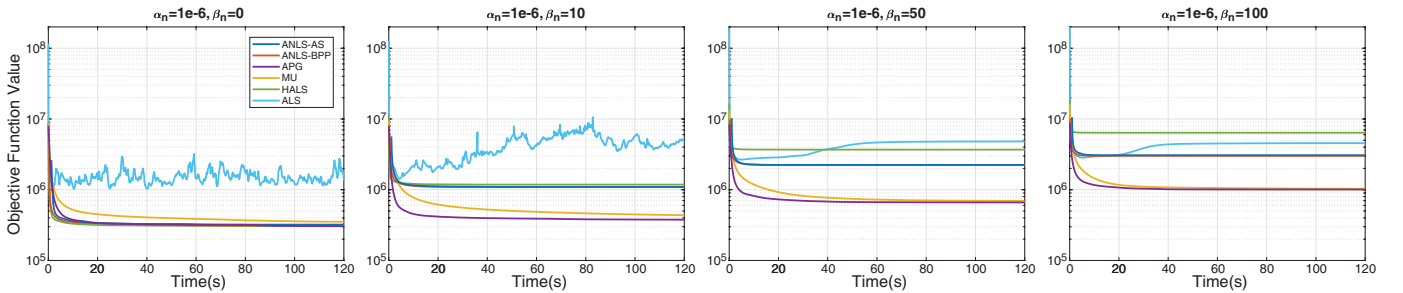


Fig. 6. The Objective Function Value Curves of Sparse NCPs on Third-order ERP Tensor With Fixed Time Limit of 120s.

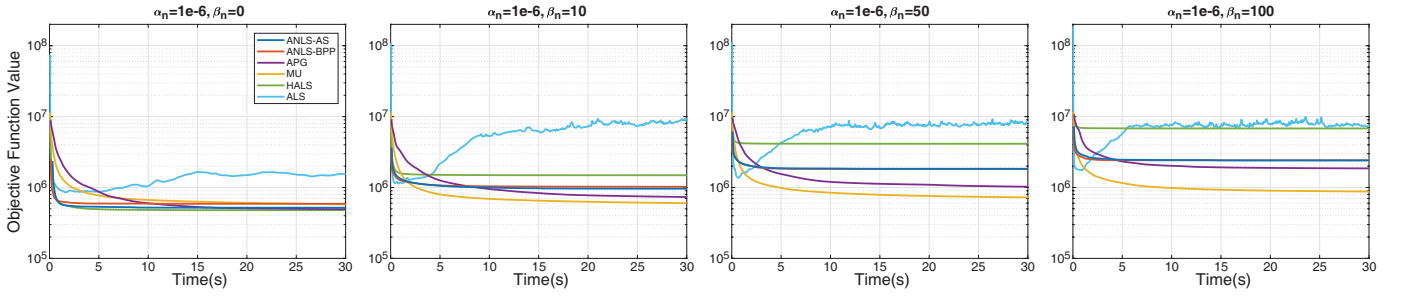


Fig. 7. The Objective Function Value Curves of Sparse NCPs on Fourth-order ERP Tensor With Fixed Time Limit of 30s.

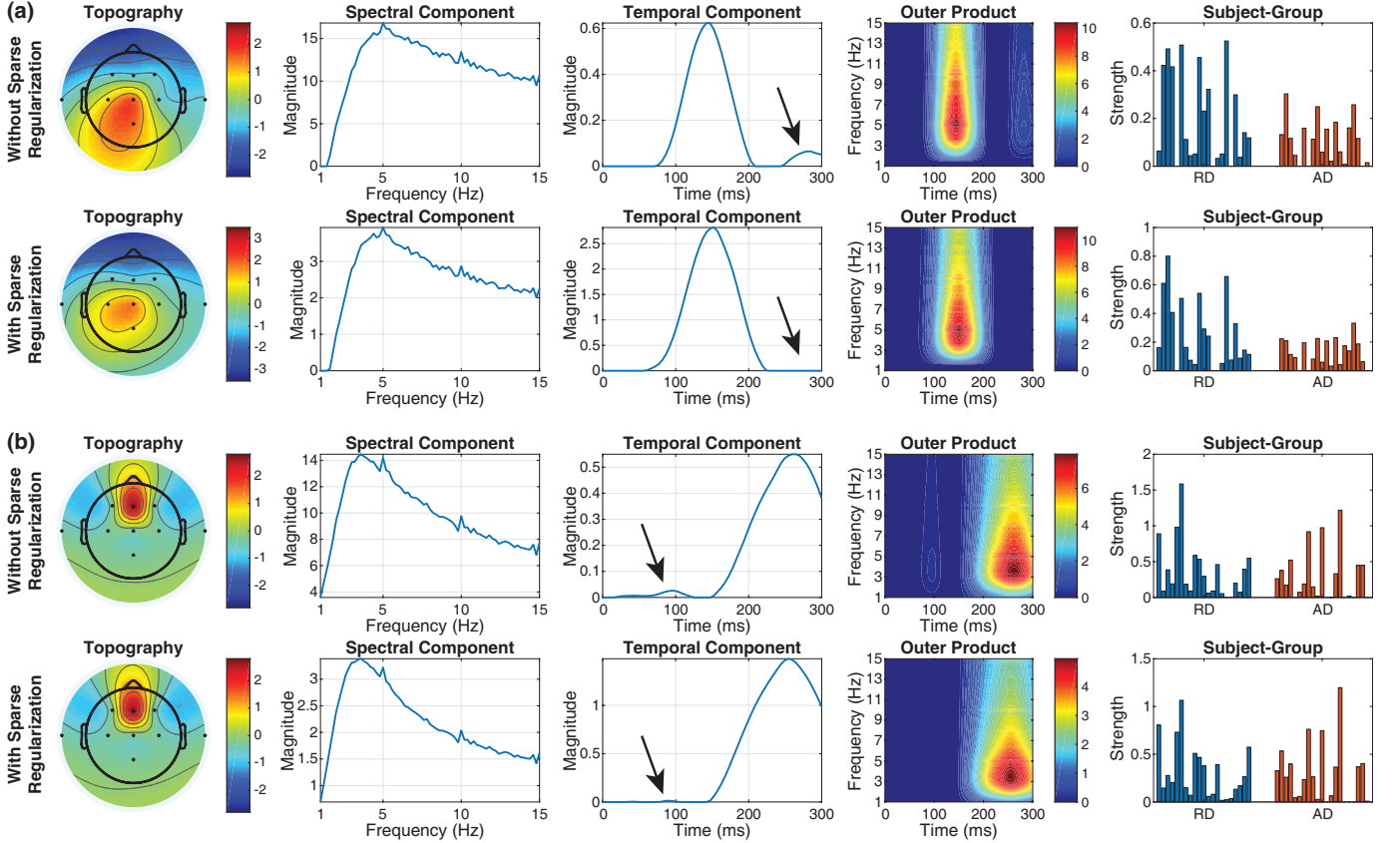


Fig. 8. Selected components from the fourth-order ERP tensor without and with sparse regularization. The top components in (a) and (b) were extracted using original APG method. The bottom components in (a) and (b) were extracted from sparsity regularized APG with  $\beta_n = 10$ .

in subsection V-C. For this experiment, the maximum running time was set by 120 seconds. Other settings are the same as those in the third-order case. We recorded the values of objective function, relative error, running time, iteration number, the sparsity level and nonzero component number of the temporal factor matrix. The average values after 30 times of run are recorded in **Table II**. We also recorded the objective function values of all methods with  $\beta_n = 0, 10, 50, 100$  within the first 30 seconds as shown in **Fig. 7**.

For ANLS-AS, ANLS-BPP, MU, HALS and ALS, the results of the fourth-order ERP tensor in **Table II** and **Fig. 7** reveal similar properties as those in the third-order case. For the fourth-order case, MU is not very effective to impose sparsity on the factor matrices, whose sparsity are very close to the results without sparse regularization. Hence MU has

smaller relative error and lower objective function value as shown in **Fig. 7**. However, APG minimizes the objective function slowly even than MU for the fourth-order ERP tensor, which is quite different from the situation in the third-order case.

Despite the slow decrease of the objective function, APG can guarantee to converge and has exhibited effectiveness to impose sparsity. Two groups of components extracted by APG method without and with sparse regularization are shown in **Fig. 8**. It is clear to see from the temporal components that, with proper sparse regularization parameter  $\beta_n$  ( $\beta_n = 10$  in this case), some weak and redundant elements are suppressed.

## VI. DISCUSSION

From the results and analyses of the sparse NCP experiments, we have the following findings.

MU is a common method for NMF, although it shows slow convergence. It can also be extended to NCP due to the flexibility to handle regularization. However, MU still converges very slowly in NCP compared with other methods, which sometimes is not very sensitive to sparse regularization.

ALS method is very simple to implement, but it is not stable for NCP with sparse regularization. By ALS, the nonnegative constraint is just obtained by projecting all negative elements of factor matrices to zeros in the subproblems. Hence the solution by projecting is not an accurate solution to subproblem. Therefore, ALS method can not guarantee the convergence of NCP.

HALS is a very efficient method for NCP. Nevertheless, the required normalization procedures will complicate the optimization problem. In our experiments, we find that HALS does not perform well to impose sparsity. High objective function value and relative error occur with large sparse regularization parameters due to the normalization procedures.

APG has proved to be a convergent and stable method for tensor decomposition due to the proximal gradient, which exhibits high efficiency for third-order tensor. Meanwhile, APG can also handle sparse regularization flexibly, which yields closed-form solution. In spite of the convergence property, APG turns out very slowly for the fourth-order tensor case. In future, further studies are needed to accelerate APG for higher-order ( $\text{order} \geq 4$ ) nonnegative tensor decomposition.

ANLS framework converges fast and stably for sparse NCP benefiting from the advantages of many NNLS optimization methods, such as Active Set (AS) and Block Principal Pivoting (BPP). In addition, ANLS exhibits excellent performance to impose sparsity by tuning the sparse regularization parameter  $\beta_n$ . However, in order to be compatible with the ANLS framework, squared  $l_1$ -norm has to be employed as the sparse regularization item. Therefore, the method to impose sparsity in ANLS is slightly different from those in other sparse NCP methods. It is very interesting to find the way to solve sparse NCP with non-squared  $l_1$ -norm by NNLS, which will further minimize the objective function value as we believe.

At last, we want to mention the convergence properties of above optimization methods. The Frobenius norm regularization in sparse NCP (4) can prevent rank deficiency of the matrix  $B^{(n)}$  in subproblem (5), which will improve the convergence of sparse NCP to a globally optimal solution [51]. ANLS-BPP and ALS method require the  $B^{(n)}$  to be of full rank [12], while the methods of ANLS-AS, APG, HALS and MU don't require the full rank condition. Both ANLS framework and APG method have very good convergence properties, which have been explained in [12] and [13] respectively. The subproblem of HALS method has closed form solution [12], but the normalization procedures might spoil the convergence property of HALS [22]. In addition, the convergence of MU and ALS can't be guaranteed. We don't make deep analysis of the convergence properties of these optimization methods in this paper. More information about the convergence properties

of the general block coordinate descent (BCD) method can be found in [14].

## VII. CONCLUSION

In this paper, we investigated CANDECOMP/PARAFAC tensor decomposition with both nonnegative constraint and sparse regularization (sparse NCP). The methods of MU, ALS, HALS, APG and ANLS in block coordinate descent framework were deeply analyzed to solve sparse NCP. We compared all these methods by experiments on synthetic and real tensor data, both of which contain third-order and fourth-order cases. We find that APG and ANLS methods are stably convergent and highly effective to impose sparsity for the tensor decomposition compared with other methods. Meanwhile, ANLS framework is very efficient to process higher-order ( $\text{order} \geq 4$ ) tensor data. The proposed accelerated method to compute the objective function and relative error had further improved the efficiency of the sparse NCP.

## REFERENCES

- [1] A. Cichocki, R. Zdunek, A. H. Phan, and S.-i. Amari, *Nonnegative matrix and tensor factorizations: applications to exploratory multi-way data analysis and blind source separation*. John Wiley & Sons, 2009.
- [2] Y.-X. Wang and Y.-J. Zhang, "Nonnegative matrix factorization: A comprehensive review," *IEEE Transactions on Knowledge and Data Engineering*, vol. 25, no. 6, pp. 1336–1353, jun 2013.
- [3] G. Zhou, A. Cichocki, Q. Zhao, and S. Xie, "Nonnegative matrix and tensor factorizations: An algorithmic perspective," *IEEE Signal Processing Magazine*, vol. 31, no. 3, pp. 54–65, may 2014.
- [4] D. D. Lee and H. S. Seung, "Learning the parts of objects by non-negative matrix factorization," *Nature*, vol. 401, no. 6755, pp. 788–791, oct 1999.
- [5] W. He, H. Zhang, and L. Zhang, "Total variation regularized reweighted sparse nonnegative matrix factorization for hyperspectral unmixing," *IEEE Transactions on Geoscience and Remote Sensing*, vol. 55, no. 7, pp. 3909–3921, jul 2017.
- [6] M. A. Veganzones, J. E. Cohen, R. C. Farias, J. Chanussot, and P. Comon, "Nonnegative tensor CP decomposition of hyperspectral data," *IEEE Transactions on Geoscience and Remote Sensing*, vol. 54, no. 5, pp. 2577–2588, may 2016.
- [7] M. Mørup, L. K. Hansen, J. Parnas, and S. M. Arnfred, "Decomposing the time-frequency representation of EEG using non-negative matrix and multi-way factorization," *Technical University of Denmark Technical Report*, 2006. [Online]. Available: [http://www2.imm.dtu.dk/pubdb/views/edoc\\_download.php/4144/pdf/imm4144.pdf](http://www2.imm.dtu.dk/pubdb/views/edoc_download.php/4144/pdf/imm4144.pdf)
- [8] F. Cong, Q.-H. Lin, L.-D. Kuang, X.-F. Gong, P. Astikainen, and T. Ristaniemi, "Tensor decomposition of EEG signals: A brief review," *Journal of Neuroscience Methods*, vol. 248, pp. 59–69, jun 2015.
- [9] S. Elcoroaristizabal, R. Bro, J. A. García, and L. Alonso, "PARAFAC models of fluorescence data with scattering: A comparative study," *Chemometrics and Intelligent Laboratory Systems*, vol. 142, pp. 124–130, mar 2015.
- [10] X. Vu, C. Chaux, N. Thirion-Moreau, S. Maire, and E. M. Carstea, "A new penalized nonnegative third-order tensor decomposition using a block coordinate proximal gradient approach: Application to 3d fluorescence spectroscopy," *Journal of Chemometrics*, vol. 31, no. 4, p. e2859, feb 2017.
- [11] M. Mørup, "Applications of tensor (multiway array) factorizations and decompositions in data mining," *Wiley Interdisciplinary Reviews: Data Mining and Knowledge Discovery*, vol. 1, no. 1, pp. 24–40, jan 2011.
- [12] J. Kim, Y. He, and H. Park, "Algorithms for nonnegative matrix and tensor factorizations: a unified view based on block coordinate descent framework," *Journal of Global Optimization*, vol. 58, no. 2, pp. 285–319, mar 2014.
- [13] Y. Xu and W. Yin, "A block coordinate descent method for regularized multiconvex optimization with applications to nonnegative tensor factorization and completion," *SIAM Journal on Imaging Sciences*, vol. 6, no. 3, pp. 1758–1789, jan 2013.

- [14] D. P. Bertsekas, *Nonlinear Programming, Third Edition*. Belmont, Massachusetts: Athena Scientific, 2016.
- [15] D. D. Lee and H. S. Seung, "Algorithms for non-negative matrix factorization," in *Advances in neural information processing systems*, 2001, pp. 556–562.
- [16] M. W. Berry, M. Browne, A. N. Langville, V. P. Pauca, and R. J. Plemmons, "Algorithms and applications for approximate nonnegative matrix factorization," *Computational Statistics & Data Analysis*, vol. 52, no. 1, pp. 155–173, sep 2007.
- [17] A. Cichocki, R. Zdunek, and S. ichi Amari, "Hierarchical ALS algorithms for nonnegative matrix and 3d tensor factorization," in *Independent Component Analysis and Signal Separation*. Springer Berlin Heidelberg, 2007, pp. 169–176.
- [18] A. Cichocki and A.-H. Phan, "Fast local algorithms for large scale nonnegative matrix and tensor factorizations," *IEICE Transactions on Fundamentals of Electronics, Communications and Computer Sciences*, vol. E92-A, no. 3, pp. 708–721, 2009.
- [19] N. Guan, D. Tao, Z. Luo, and B. Yuan, "NeNMF: An optimal gradient method for nonnegative matrix factorization," *IEEE Transactions on Signal Processing*, vol. 60, no. 6, pp. 2882–2898, jun 2012.
- [20] S. Boyd, "Distributed optimization and statistical learning via the alternating direction method of multipliers," *Foundations and Trends® in Machine Learning*, vol. 3, no. 1, pp. 1–122, 2011.
- [21] D. L. Sun and C. Fevotte, "Alternating direction method of multipliers for non-negative matrix factorization with the beta-divergence," in *2014 IEEE International Conference on Acoustics, Speech and Signal Processing (ICASSP)*. IEEE, may 2014.
- [22] C.-J. Lin, "Projected gradient methods for nonnegative matrix factorization," *Neural Computation*, vol. 19, no. 10, pp. 2756–2779, oct 2007.
- [23] R. Zdunek and A. Cichocki, "Non-negative matrix factorization with quasi-newton optimization," in *International conference on artificial intelligence and soft computing*. Springer, 2006, pp. 870–879.
- [24] D. Kim, S. Sra, and I. S. Dhillon, "Fast newton-type methods for the least squares nonnegative matrix approximation problem," in *Proceedings of the 2007 SIAM International Conference on Data Mining*. Society for Industrial and Applied Mathematics, apr 2007, pp. 343–354.
- [25] H. Kim and H. Park, "Nonnegative matrix factorization based on alternating nonnegativity constrained least squares and active set method," *SIAM Journal on Matrix Analysis and Applications*, vol. 30, no. 2, pp. 713–730, jan 2008.
- [26] J. Kim and H. Park, "Fast nonnegative matrix factorization: An active-set-like method and comparisons," *SIAM Journal on Scientific Computing*, vol. 33, no. 6, pp. 3261–3281, jan 2011.
- [27] X. Dai, C. Li, X. He, and C. Li, "Nonnegative matrix factorization algorithms based on the inertial projection neural network," *Neural Computing and Applications*, jan 2018.
- [28] C. Zhang, L. Jing, and N. Xiu, "A new active set method for nonnegative matrix factorization," *SIAM Journal on Scientific Computing*, vol. 36, no. 6, pp. A2633–A2653, jan 2014.
- [29] J. Kim and H. Park, "Fast nonnegative tensor factorization with an active-set-like method," in *High-Performance Scientific Computing*. Springer London, 2012, pp. 311–326.
- [30] A. P. Liavas and N. D. Sidiropoulos, "Parallel algorithms for constrained tensor factorization via alternating direction method of multipliers," *IEEE Transactions on Signal Processing*, vol. 63, no. 20, pp. 5450–5463, oct 2015.
- [31] K. Huang, N. D. Sidiropoulos, and A. P. Liavas, "A flexible and efficient algorithmic framework for constrained matrix and tensor factorization," *IEEE Transactions on Signal Processing*, vol. 64, no. 19, pp. 5052–5065, oct 2016.
- [32] K. Ito and A. K. Landi, "The nonnegative matrix factorization: Regularization and complexity," *SIAM Journal on Scientific Computing*, vol. 38, no. 2, pp. B327–B346, jan 2016.
- [33] D. Cai, X. He, J. Han, and T. S. Huang, "Graph regularized nonnegative matrix factorization for data representation," *IEEE Transactions on Pattern Analysis and Machine Intelligence*, vol. 33, no. 8, pp. 1548–1560, aug 2011.
- [34] R. Shang, C. Liu, Y. Meng, L. Jiao, and R. Stolkin, "Nonnegative matrix factorization with rank regularization and hard constraint," *Neural Computation*, vol. 29, no. 9, pp. 2553–2579, sep 2017.
- [35] D. Wang, X. Wang, Y. Zhu, P. Toivainen, M. Huotilainen, T. Ristaniemi, and F. Cong, "Increasing stability of EEG components extraction using sparsity regularized tensor decomposition," in *Advances in Neural Networks – ISNN 2018*. Springer International Publishing, 2018, pp. 789–799.
- [36] P. O. Hoyer, "Non-negative matrix factorization with sparseness constraints," *Journal of machine learning research*, vol. 5, no. Nov, pp. 1457–1469, 2004.
- [37] N. Mohammadiha and A. Leijon, "Nonnegative matrix factorization using projected gradient algorithms with sparseness constraints," in *2009 IEEE International Symposium on Signal Processing and Information Technology (ISSPIT)*. IEEE, dec 2009.
- [38] A. M. Bruckstein, D. L. Donoho, and M. Elad, "From sparse solutions of systems of equations to sparse modeling of signals and images," *SIAM Review*, vol. 51, no. 1, pp. 34–81, feb 2009.
- [39] D. L. Donoho, "For most large underdetermined systems of linear equations the minimal  $\ell_1$ -norm solution is also the sparsest solution," *Communications on Pure and Applied Mathematics*, vol. 59, no. 6, pp. 797–829, 2006.
- [40] P. O. Hoyer, "Non-negative sparse coding," in *Proceedings of the 12th IEEE Workshop on Neural Networks for Signal Processing*. IEEE, 2002.
- [41] J. Xuan, J. Lu, G. Zhang, R. Y. D. Xu, and X. Luo, "Doubly non-parametric sparse nonnegative matrix factorization based on dependent indian buffet processes," *IEEE Transactions on Neural Networks and Learning Systems*, vol. 29, no. 5, pp. 1835–1849, may 2018.
- [42] M. Mørup, L. K. Hansen, and S. M. Arnfred, "Algorithms for sparse nonnegative Tucker decompositions," *Neural Computation*, vol. 20, no. 8, pp. 2112–2131, aug 2008.
- [43] J. Liu, J. Liu, P. Wonka, and J. Ye, "Sparse non-negative tensor factorization using columnwise coordinate descent," *Pattern Recognition*, vol. 45, no. 1, pp. 649–656, jan 2012.
- [44] Y. Xu, "Alternating proximal gradient method for sparse nonnegative Tucker decomposition," *Mathematical Programming Computation*, vol. 7, no. 1, pp. 39–70, may 2015.
- [45] T. G. Kolda and B. W. Bader, "Tensor decompositions and applications," *SIAM Review*, vol. 51, no. 3, pp. 455–500, aug 2009.
- [46] B. W. Bader and T. G. Kolda, "Efficient MATLAB computations with sparse and factored tensors," *SIAM Journal on Scientific Computing*, vol. 30, no. 1, pp. 205–231, jan 2008.
- [47] B. W. Bader, T. G. Kolda *et al.*, "Matlab tensor toolbox version 2.6," Available online, February 2015. [Online]. Available: <http://www.sandia.gov/~tgkolda/TensorToolbox/>
- [48] B. W. Bader and T. G. Kolda, "Algorithm 862: MATLAB tensor classes for fast algorithm prototyping," *ACM Transactions on Mathematical Software*, vol. 32, no. 4, pp. 635–653, dec 2006.
- [49] M. E. Timmerman and H. A. L. Kiers, "Three-mode principal components analysis: Choosing the numbers of components and sensitivity to local optima," *British Journal of Mathematical and Statistical Psychology*, vol. 53, no. 1, pp. 1–16, may 2000.
- [50] F. Cong, A. H. Phan, Q. Zhao, T. Huttunen-Scott, J. Kaartinen, T. Ristaniemi, H. Lyytinen, and A. Cichocki, "Benefits of multi-domain feature of mismatch negativity extracted by non-negative tensor factorization from eeg collected by low-density array," *International Journal of Neural Systems*, vol. 22, no. 06, p. 1250025, dec 2012.
- [51] L.-H. Lim and P. Comon, "Nonnegative approximations of nonnegative tensors," *Journal of Chemometrics*, vol. 23, no. 7-8, pp. 432–441, jul 2009.